1   Factors affecting B/Ca ratios in synthetic aragonite

2

3   M. Holcomb[1,2,3*], T.M. DeCarlo[4], G.A. Gaetani[5], M. McCulloch[1,2]

4

5   [1]The UWA Oceans Institute and School of Earth and Environment, The University of

6   Western Australia, Crawley 6009, WA, Australia.

7

8   [2]ARC Centre of Excellence in Coral Reef Studies, The University of Western Australia,

9   Crawley 6009, WA, Australia.

10

11   [3]Centre Scientifique de Monaco, Monaco, Principality of Monaco

12

13   [4]Massachusetts Institute of Technology/Woods Hole Oceanographic Institution Joint

14   Program in Oceanography/Applied Ocean Physics and Department of Marine Geology

15   and Geophysics, Woods Hole, MA 02543, U.S.A.

16   [5] Woods Hole Oceanographic Institution, Department of Marine Geology and

17   Geophysics, Woods Hole, MA 02543, U.S.A.

18

19   *Corresponding author: mholcomb3051@gmail.com

20

21   Keywords: Boron; aragonite; coral; proxy; carbonate

22 **Abstract**

23 Measurements of B/Ca ratios in marine carbonates have been suggested to record

24 seawater carbonate chemistry, however experimental calibration of such proxies based on

25 inorganic partitioning remains limited. Here we conducted a series of synthetic aragonite

26 precipitation experiments to evaluate the factors influencing the partitioning of B/Ca

27 between aragonite and seawater. Our results indicate that the B/Ca ratio of synthetic

28 aragonites depends primarily on the relative concentrations of borate and carbonate ions

29 in the solution from which the aragonite precipitates; not on bicarbonate concentration as

30 has been previously suggested. The influence of temperature was not significant over the

31 range investigated (20 – 40 $^{\circ}$C), however, partitioning may be influenced by saturation

32 state (and/or growth rate). Based on our experimental results, we suggest that aragonite

33 B/Ca ratios can be utilized as a proxy of $[CO_3^{2-}]$. Boron isotopic composition (δ^{11}B) is an

34 established pH proxy, thus B/Ca and δ^{11}B together allow the full carbonate chemistry of

35 the solution from which the aragonite precipitated to be calculated. To the extent that

36 aragonite precipitation by marine organisms is affected by seawater chemistry, B/Ca may

37 also prove useful in reconstructing seawater chemistry. A simplified boron purification

38 protocol based on amberlite resin and the organic buffer TRIS is also described.

39

40 **1. Introduction**

41   Boron concentrations and boron isotopic compositions in marine carbonates are

42 potential archives of past seawater pH and carbonate chemistry (e.g. Sanyal et al., 1996;

43 Pelejero et al., 2005; Pearson and Palmer, 1999; Douville et al., 2010; Rae et al., 2011;

44 Henehan et al., 2013; Penman et al., 2013).   In seawater, boron is typically present in

45 two forms, boric acid ($B(OH)_3$) and borate ($B(OH)_4^-$), the relative abundances of which

46 depend largely on pH (e.g. Culberson, 1968; Dickson, 1990; Klochko et al., 2006). The

47 $B(OH)_4^-$ ion is thought to be the primary form of boron incorporated into calcium

48 carbonate (e.g. Sen et al., 1994; Hemming et al., 1995), thus offering the potential to use

49 B/Ca ratios to estimate pH and/or carbonate chemistry (e.g. Yu et al., 2007). However,

50 there is uncertainty as to how boron incorporation may depend upon concentrations of

51 different dissolved inorganic carbon (DIC) species (e.g. Hemming et al., 1995; Uchikawa

52 et al., 2015). In addition, there are suggestions that $B(OH)_3$ may also be incorporated,

53 especially in calcite (e.g. Xiao et al., 2008; Klochko et al., 2009; Rollion-Bard et al.,

54 2011; Mavromatis et al., 2015; Uchikawa et al., 2015), thus potentially complicating the

55 interpretation of B/Ca ratios.

56 Various relationships have been used to explore the range of possible factors

57 controlling B incorporation in both synthetic (e.g. Mavromatis et al., 2015; Uchikawa et

58 al., 2015) and biogenic carbonates (e.g. Ni et al., 2007; Yu et al., 2007; Yu and

59 Elderfield, 2007; Foster 2008; Douville et al., 2010; Allen et al., 2011; Rae et al., 2011;

60 Tripati et al., 2011; Allen et al., 2012; Allison et al., 2014; Babila et al., 2014; Henehan et

61 al., 2015). Here we consider several of the relationships proposed by previous studies:

62 $B(OH)_4^-/CO_3^{2-}$, $B(OH)_4^-/HCO_3^-$, $B(OH)_4^-/(CO_3^{2-} + HCO_3^-)$, B/HCO_3^-, $B/(CO_3^{2-} + HCO_3^-)$,

63 $B(OH)_4^-/\Delta CO_3^{2-}$ (where ΔCO_3^{2-} is the difference between the actual $[CO_3^{2-}]$ and the

64 $[CO_3^{2-}]$ at which the solution would be saturated with respect to aragonite, $\Omega_{Arag} = 1$). In

65 addition to various empirical relationships, we also consider potential balanced exchange

66 reactions with the following expressions for the distribution coefficient:
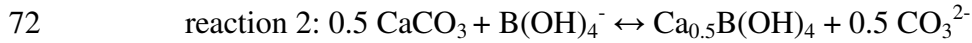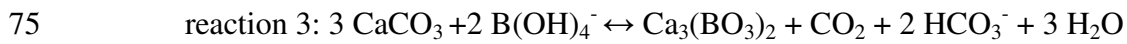
67

68   reaction 1 (Hemming and Hanson 1992):

69         $CaCO_3 + B(OH)_4^- \leftrightarrow Ca(HBO_3) + HCO_3^- + H_2O$
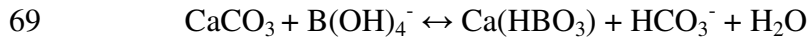
70
$$K_D = \frac{[HBO_3^{2-}/CO_3^{2-}]_{CaCO_3}}{[B(OH)_4^-/HCO_3^-]_{solution}}$$
       eq. 1

71

72   reaction 2: $0.5\ CaCO_3 + B(OH)_4^- \leftrightarrow Ca_{0.5}B(OH)_4 + 0.5\ CO_3^{2-}$

73
$$K_D = \frac{[B(OH)_4^-/[CO_3^{2-}]^{0.5}]_{CaCO_3}}{[B(OH)_4^-/[CO_3^{2-}]^{0.5}]_{solution}}$$
       eq. 2

74

75   reaction 3: $3\ CaCO_3 + 2\ B(OH)_4^- \leftrightarrow Ca_3(BO_3)_2 + CO_2 + 2\ HCO_3^- + 3\ H_2O$

76
$$K_D = \frac{[[BO_3^{3-}]^2/[CO_3^{2-}]^3]_{CaCO_3}}{[[B(OH)_4^-]^2/[CO_2][HCO_3^-]^2]_{solution}}$$
       eq. 3

77   Studies of naturally formed samples do provide some insights into the potential

78 controls on boron incorporation (Hemming and Hanson 1992; Sanyal et al., 1996; Wara

79 et al., 2003; Ni et al., 2007; Yu et al., 2007; Yu and Elderfield, 2007; Foster et al., 2008;

80 Rollion-Bard et al., 2011; Allison et al., 2014; Kaczmarek et al., 2015). However, such

81 studies cannot establish how B/Ca is controlled by environmental variables due to

82 inevitable uncertainty as to the conditions during carbonate deposition. This is

83 particularly the case for calcifying organisms that modify the conditions at the site of

84 calcification substantially from the conditions present in the surrounding seawater (e.g.

85 Al-Horani et al., 2003; McCulloch et al., 2012; De Nooijer et al., 2014). Since the

86 chemistry at the site of calcification is generally unknown, most studies have focused on

87 the relationship between B/Ca and seawater chemistry. Thus in studies of biologically

88   formed calcium carbonate, there is uncertainty as to whether B/Ca changes in direct

89   response to environmental conditions, or if it reflects physiological changes in the

90   organism.

91   Laboratory studies on the incorporation of B into calcium carbonate remain

92   limited, and few potentially controlling factors (e.g. temperature, carbonate chemistry,

93   growth rate etc) have been tested (Kitano et al., 1978; Sen et al. 1994; Hemming et al.,

94   1995; Hobbs and Reardon, 1999; Sanyal et al., 2000; Xiao et al., 2008; He et al., 2013;

95   Gabitov et al., 2014; Mavromatis et al., 2015; Uchikawa et al., 2015). Critically only one

96   study has characterized the carbonate chemistry during aragonite precipitation

97   (Mavromatis et al., 2015).

98   We conducted a series of experiments to explore how carbonate chemistry,

99   organic additives, temperature, and boron concentration may influence B/Ca ratios in

100   aragonite formed from seawater-like solutions. Manipulation of pH, DIC, and Ca^{2+} are

101   among the mechanisms potentially driving biogenic calcification, thus our experiments

102   focused on manipulating these variables. In addition to these inorganic variables, there

103   are also a wide range of organic molecules produced by calcifying organisms which may

104   influence calcification (e.g. Mass et al., 2013). We chose to test one specific mechanism

105   by which organic molecules could influence B/Ca, that of buffering pH. In seawater, the

106   two dominant pH buffers are DIC and B species, thus variations in pH (such as might

107   occur adjacent to a growing aragonite crystal) would directly affect DIC and B

108   speciation. By adding an additional buffering agent (such as 2-Amino-2-hydroxymethyl-

109   propane-1,3-diol (TRIS) or 4-(2-hydroxyethyl)-1-piperazineethanesulfonic acid

110   (HEPES)), pH could in theory be more stable adjacent to the growing crystal which could

111   alter the relationship between B/Ca and bulk solution chemistry. In addition to biological

112   processes affecting elemental ratios, there is also a potential for some of the compounds

113   used to study crystal growth to influence elemental incorporation. Calcein is among the

114   molecules commonly used to mark growing crystals in living organisms (e.g. Venn et al.,

115   2013), and the influence of calcein on the incorporation of a number of elements has been

116   tested (Dissard et al., 2009), though no information is thus-far available as the effect of

117   calcein on B/Ca, thus it was tested here.

118

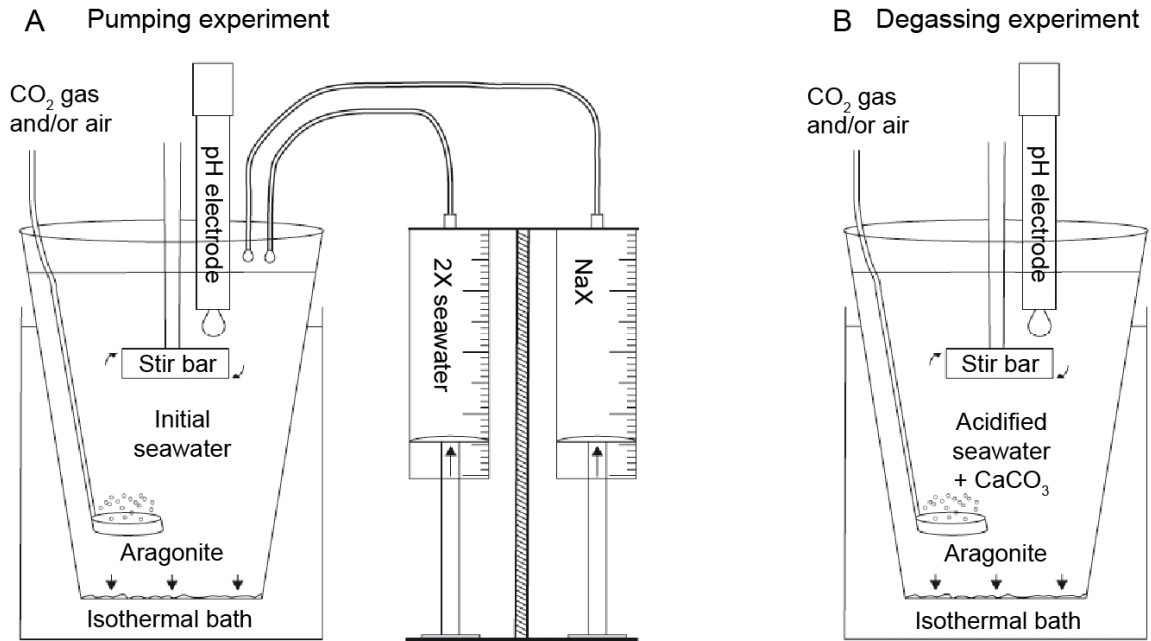119   **2. Methods**

120   *2.1. Aragonite precipitation*

121   Aragonite was precipitated from seawater (0.2 µm filtered to remove living

122   organisms) using several different approaches adapted from existing methods (Kinsman

123   and Holland 1969; Kitano et al., 1978; Gaetani and Cohen 2006; Holcomb et al., 2009;

124   Gabitov et al., 2011; Wang et al., 2013). The range of experimental protocols used was

125   intended to precipitate aragonite under a wide range of solution chemistries in order to

126   encompass the likely compositional range of biologically mediated solutions and thus

127   more fully evaluate the factors that affect boron incorporation during bio-calcification.

128   Detailed descriptions of the protocols used for each of the 65 experiments are provided in

129   the supplementary materials (see section S1 and Table S1 for more details). Briefly, all

130   experiments were carried out in plastic containers held within constant temperature water

131   baths. Two general types of experiments were conducted: degassing (Figure 1B) and

132   pumping (Figure 1A) experiments. Degassing experiments were carried out by

133   dissolving $CaCO_3$ in seawater at ~1 atm pCO_2 with the addition of $MgCl_2$, $SrCO_3$ (to

134   maintain seawater like Mg/Ca and Sr/Ca ratios) and various additives (TRIS, HEPES,

135   calcein, boron, $CaCl_2$, etc. depending upon the experiment). As CO_2 degassed in these

136   experiments, Ω_{Arag} increased until aragonite began to precipitate. Degassing experiments

137   were bubbled at controlled rates with air or air/CO_2 mixes during precipitation to stabilize

138   pH. Pumping experiments were conducted by adding seawater containing $CaCO_3$

139   (dissolved by bubbling with CO_2) or concentrated seawater (evaporated to achieve 2x

140   normal salinity = 2xsw) and a $NaHCO_3$ or Na_2CO_3 or NaOH or mixture there-of solution

141   (here after referred to as NaX solution) to seawater using a syringe pump. The

142   simultaneous injection of 2xsw and NaX solutions allowed carbonate chemistry to be

143   modified while maintaining salinity ~constant. Pumping rates were varied over the

144   course of each experiment to stabilize pH during precipitation. Some of these

145   experiments were additionally bubbled with air or air/CO_2 mixtures, and some contained

146   additional additives. All experiments were stirred continuously.

147   The evolution of solution chemistry during precipitation differed among

148   experiments. In general, in pumping experiments an initial pH and alkalinity was

149   established, precipitation then removed CO_3^{2-} thus reducing DIC (or equivalently total

150   inorganic carbon) and alkalinity, while pumping of the NaX solution added DIC and

151   alkalinity, thus allowing carbonate chemistry to be maintained nearly constant during

152   precipitation. In degassing experiments, though pH was maintained nearly constant,

153   DIC, and alkalinity both declined during precipitation due to the precipitate removing

154   DIC and alkalinity and bubbling removing DIC. To illustrate the relationships between

155   different solution chemistry parameters potentially relevant for B/Ca, Figure 2 shows

156　　various chemical parameters plotted versus pH_T for our experiments, as well as the values

157　　expected for seawater at different DIC concentrations.

158

A Pumping experiment　　　　　　　　　　　　　　**B** Degassing experiment

CO$_2$ gas and/or air — pH electrode — Stir bar — Initial seawater — 2X seawater — NaX — Aragonite — Isothermal bath

CO$_2$ gas and/or air — pH electrode — Stir bar — Acidified seawater + CaCO$_3$ — Aragonite — Isothermal bath

159

160　　Figure 1. Schematic representation of the experimental setup used for pumping (A) and

161　　degassing (B) experiments.

162

163   Over the course of each experiment, samples were taken for pH, alkalinity, and

164 solution chemistry measurements. Samples for alkalinity and solution chemistry were

165 filtered (Millex-HV syringe filter, 0.45 μm PVDF membrane) at the time of collection to

166 remove any aragonite particles potentially present. All seawater samples used for

167 elemental composition measurements were acidified with concentrated HNO_3 to dissolve

168 any material that precipitated post-collection. Details of all measurements, associated

169 calculations, and measured values are provided in the supplementary materials (sections

170 S2, S3, and .xls file).

171

172 *2.2. Precipitate Characterization*

173 *2.2.1. Mineralogy*

174 The mineralogy of most experiments was characterized by XRD (see supplemental

175 materials section S4) and/or Raman spectroscopy (DeCarlo et al., 2015; and supplemental

176 materials S4). Some experiments contained phases other than aragonite and were

177 generally excluded from analysis of B/Ca, with the exception of one sample (10h) which

178 had a faint XRD peak near 2-theta = 30, suggesting possible contamination with a calcitic

179 phase, but neither the Raman spectra nor the elemental composition indicated a non-

180 aragonitic phase, thus any contamination was assumed to be sufficiently low as to not

181 compromise the use of the sample.

182

183 *2.2.2. Composition*

184   The elemental composition of all precipitates was measured using Q-ICPMS

185   (supplemental materials S3.1) to verify that the elemental composition was similar to

186   other marine aragonite samples while simultaneously measuring the B/Ca ratio. The

187   coral standard JCp-1 (B/Ca = 0.4596 mmol mol^{-1}, Hathorne et al. (2013)) was used to

188   standardize all measurements, and the validity of this approach for measuring B/Ca was

189   verified using independent measurements of purified boron extracts measured via MC-

190   ICPMS (supplemental materials S3.2.1). Data on the incorporation of Sr/Ca and U/Ca

191   into these precipitates is published elsewhere (DeCarlo et al., 2015).

192

193   *2.3. Solution Characterization*

194   Since natural seawater was used for all experiments, and Ca and B are generally

195   considered uniformly distributed throughout the oceans in proportion to salinity,

196   concentrations were calculated based on salinity and the mass of any added B- or Ca-

197   containing solutions. For a subset of experiments the validity of this assumption was

198   verified via ICP-MS measurements. Measurements are described in the supplemental

199   materials including the description of new simplified chemistry for the purification of

200   boron based on amberlite IRA 743 resin and the organic buffer TRIS (supplemental

201   material S3.3).

202

203   *2.4. Calculations*

204   Carbonate chemistry was calculated using the measured alkalinity, pH, and temperature.

205   When pH measurements were carried out at a temperature different from that of the

206   experimental temperature, the pH at the experimental temperature was calculated using

207   CO2Sys (van Heuven et al., 2009). Salinities were interpolated based on initial and final

208   salinities and estimated evaporation rates. Calcium and boron concentrations in the fluid

209   were calculated based on salinity, estimated amount of precipitate deposited, and any

210   calcium or boron added to the experiment. These experiments were undertaken in

211   conjunction with those reported by DeCarlo et al. (2015), further details are given in the

212   supplemental materials (S2), as are alternative calculations using constants from Hain et

213   al. (2015) (S6).

214   Since aragonite is primarily $CaCO_3$, and thus $Ca \approx CO_3$, B/Ca can be substituted

215   for B/CO_3 when calculating distribution coefficients, so though equations 1-3 are

216   expressed relative to CO_3 in the solid, B/Ca will be used for calculations.

217

218   *2.5. Average solution chemistry and partitioning*

219   We evaluated the factors controlling B incorporation into aragonite by comparing the

220   bulk/mean aragonite B/Ca ratio to the average solution composition during precipitation

221   of each of 58 experiments conducted in 2013 (of 65 total experiments). The solution

222   chemistry and bulk precipitation rates varied over the course of each experiment. To

223   estimate the average solution chemistry during the time that aragonite precipitated,

224   chemistry parameters were weighted by the amount of precipitate formed over the given

225   time interval (estimated from the difference between measured and expected alkalinity).

226   The distribution coefficient relationship that best described the data was then used to

227   calculate distribution coefficients for each individual experiment such that the calculated

228   B/Ca ratio for the final precipitate in each experiment matched the measured ratio. Data

229   from experiments run in 2011 (denoted by a '/11' in the experiment name in the

230   supplemental tables) were not included in these comparisons as carbonate chemistry was

231   generally less stable; experiments from 2011 were used only for assessing the effects of

232   calcein.

233

234   *3. Results*

235   Aragonite was precipitated over a wide range of pH_T (7.3 to 9.3, where pH_T is pH

236   measured on the total scale), temperature (~20 ^{o}C to 40 ^{o}C), and carbonate chemistry

237   conditions (Fig. 2). Within any given experiment, the precipitate formed under a range of

238   solution chemistry conditions, but the range within an experiment was generally small

239   relative to the differences among experiments (Fig. 2). For example, the within-

240   experiment pH variation was typically less than 0.1 pH units, whereas among

241   experiments pH differences of more than 2 pH units were achieved. Likewise, within the

242   course of an experiment, the relative standard deviation (RSD) of $[B(OH)_4^-]/[CO_3^{2-}]^{0.5}$

243   was less than 15% (typically less than 5%), while different experiments differed by more

244   than an order of magnitude (Figure 2H, Table S2).

245   The B/Ca ratio in the precipitate showed no significant ($p > 0.05$) correlation with pH_T or

246   any single carbonate chemistry parameter. Significant ($p < 0.001$) correlations were

247   found between B/Ca and the mean solution [B] and $[B(OH)_4^-]$ (Table 1). However, when

248   considering only precipitates formed under seawater boron concentrations, B/Ca does

249   correlate significantly with a number of carbonate system parameters, most notably pH

250   and parameters closely correlated with pH (e.g. DIC species and $[B(OH)_4^-]$; Figure 3,

251   Table 1), with $[B(OH)_4^-]$ remaining the single parameter most strongly correlated with

252   B/Ca.

253

254
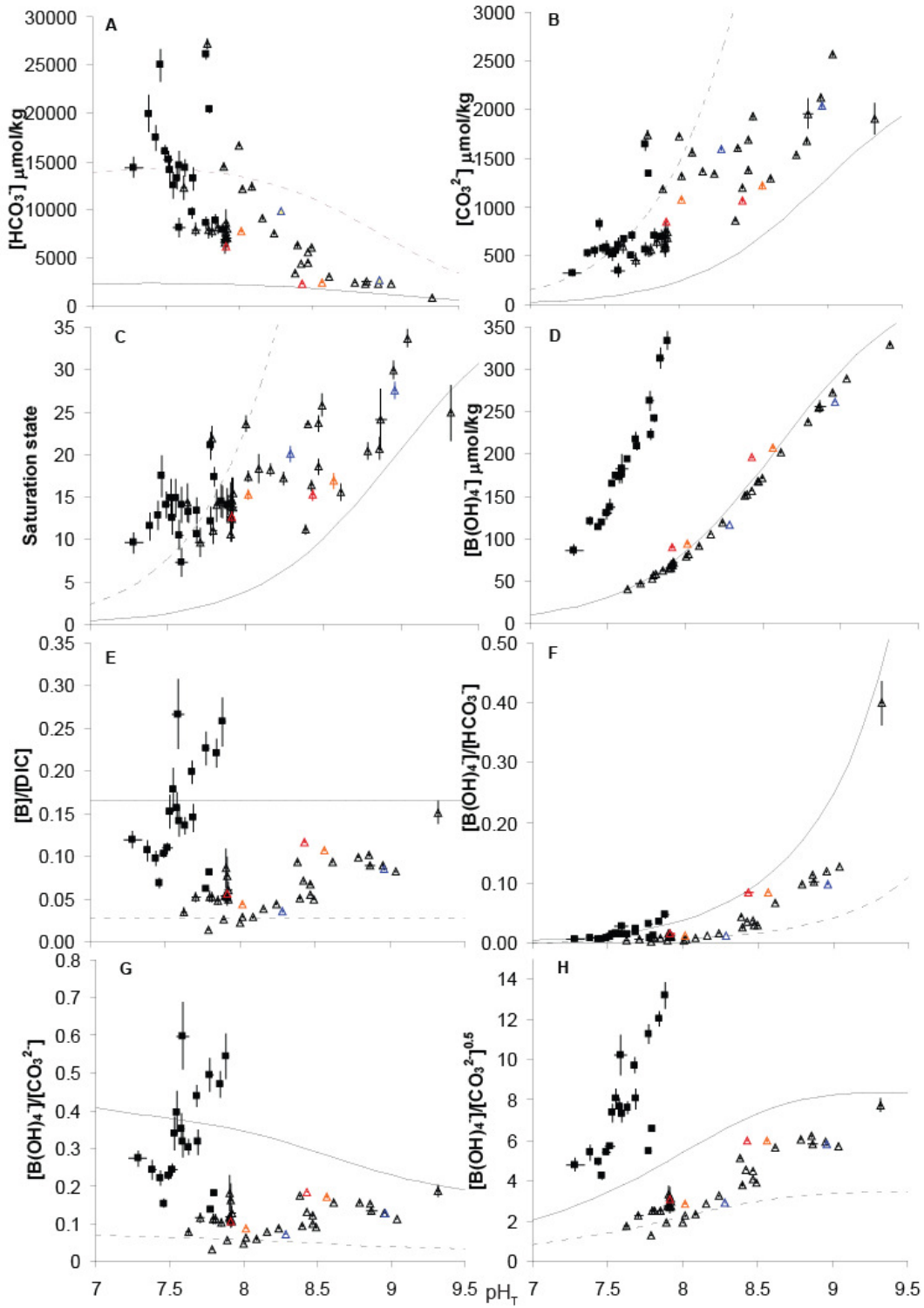
255

256   Figure 2. Relationship between different solution chemistry parameters and pH_T (total

257   scale pH) Symbols are means of individual experiments; experiments without added B

258   are represented by triangles, experiments with added B are represented by squares, lines

259   show bi-direction error bars (1 standard deviation (sd)). Experiments conducted at

260   different temperatures are shown in different colors: blue ~ 20, black ~ 25, orange ~ 33,

261   and red ~ 40 ^{o}C. Most experiments were conducted at ~ 25 ^{o}C, 2 experiments were run at

262   each of the other temperatures. Lines show calculated concentrations of different DIC

263   species and borate (μmol/kg sw) as a function of seawater pH_T. Calculated values are for

264   seawater (S=35, T=25 ^{o}C) with either 2500 (solid line) or 15000 (dashed line) μmol

265   DIC/kg sw.

266   Table 1. Pearson correlation coefficients for mean solution chemistry parameters

267   showing the most significant correlations with the B/Ca ratio of the precipitate, as well as

268   various proposed ratios suggested to be linked to B/Ca regardless of significance.

269   Correlation coefficients are given for the data set as a whole (n=58, excluding

270   experiments run in 2011), for experiments without added B (n=39), and for pumping

271   experiments without added B (n=28).   Significant (p<0.05) individual correlations are

272   indicated by [*].

Species in solution	Correlation with precipitate B/Ca		
	All experiments	Experiments with seawater [B]	Pumping experiments with seawater [B]
pH_T	0.03	0.80[*]	0.81[*]
$[HCO3^-]$	-0.16	-0.80[*]	-0.81[*]
DIC	-0.18	-0.77[*]	-0.80[*]
$[B(OH)_4^-]^2 /[CO_2][HCO_3^-]^2$	0.19	0.46[*]	0.47[*]
$[B(OH)_4^-]/[HCO_3^-]$	0.33[*]	0.77[*]	0.76[*]
$[B(OH)_4^-]/([CO_3^{2-}] + [HCO_3^-])$	0.47[*]	0.90[*]	0.90[*]
$[B(OH)_3]$	0.55[*]	-0.82[*]	-0.83[*]
$[B]/[Ca]$	0.58[*]	0.38[*]	0.23
$[B]$	0.62[*]	-0.41[*]	-0.35
$[B(OH)_4^-]/\Delta CO_3^{2-}$	0.78[*]	0.70[*]	0.92[*]
$[B(OH)_4^-]$	0.79[*]	0.82[*]	0.83[*]
$[B]/[HCO_3^-]$	0.81[*]	0.84[*]	0.85[*]
$[B(OH)_4^-]/[CO_3^{2-}]$	0.83[*]	0.81[*]	0.93[*]
$[B]/([CO_3^{2-}] + [HCO_3^-])$	0.89[*]	0.93[*]	0.97[*]
$[B]/[DIC]$	0.89[*]	0.94[*]	0.97[*]
$[B(OH)_4^-]*[Ca^{2+}]$	0.92[*]	0.82[*]	0.81[*]
$[B(OH)_4^-]/[CO_3^{2-}]^{0.5}$	0.95[*]	0.94[*]	0.95[*]

273

274

275   Since boron is thought to compete with DIC species for incorporation into aragonite (e.g.

276   Hemming et al., 1992), correlations between precipitate B/Ca and various solution

277 boron/DIC relationships were explored (Table 1). In the full data-set, B/Ca and mean

278 $[B(OH)_4^-]/[HCO_3^-]$ were not strongly correlated (Fig. 3b, based on equation 1), nor were

279 the residuals of a $[B(OH)_4^-]$ vs B/Ca regression and $[HCO_3^-]$. Nor was there a significant

280 correlation between B/Ca and average $[B(OH)_4^-]^2/[CO_2][HCO_3^-]^2$ (equation 3). B/Ca in

281 the precipitate was most strongly correlated with the mean $[B(OH)_4^-]/[CO_3^{2-}]^{0.5}$ (equation

282 2), [B]/[DIC] or $[B]/([CO_3^{2-}] + [HCO_3^-])$ and $[B(OH)_4^-]*[Ca^{2+}]$ (Table 1, Fig. 3). The

283 correlations of B/Ca with $[B(OH)_4^-]/[CO_3^{2-}]^{0.5}$ and [B]/[DIC] or $[B]/([CO_3^{2-}] + [HCO_3^-])$

284 were important regardless of whether B was added or whether only pumping or degassing

285 experiments were considered. Conversely $[B(OH)_4^-]*[Ca^{2+}]$, though significantly

286 correlated with B/Ca, did not necessarily correlate more strongly than $[B(OH)_4^-]$ alone

287 (Table 1). When only a subset of the experiments is considered, some of the other

288 potential relationships become significant (Table 1). For instance, $[B(OH)_4^-]/[CO_3^{2-}]$ is

289 highly correlated with B/Ca, especially for pumping experiments, as is $[B(OH)_4^-]/[CO_3^{2-}$

290 $]^{0.5}$, yet these two ratios show opposite behaviors in seawater as a function of pH (Fig.

291 2G,H). Given the range of DIC (2.8 – 29 mmol/kg sw) and [B] (0.39 – 2.1 mmol/kg sw)

292 among experiments (Table S2), DIC and [B] would be expected to have a greater

293 influence on $[B(OH)_4^-]/[CO_3^{2-}]$ and $[B(OH)_4^-]/[CO_3^{2-}]^{0.5}$ than pH, thus a positive

294 correlation is expected. Similarly mean $[B(OH)_4^-]/[CO_3^{2-}]^{0.5}$ and [B]/[DIC] were highly

295 correlated (Pearson correlation coefficient: 0.954) as would be expected given the large

296 ranges of DIC and [B] and their consequent influence on $[B(OH)_4^-]/[CO_3^{2-}]^{0.5}$ (e.g. Fig.

297 2). Since DIC is nearly equivalent to $[CO_3^{2-}] + [HCO_3^-]$, no separate treatment will be

298 given of the $[B]/([CO_3^{2-}] + [HCO_3^-])$ relationship. Linear least squares regression

299 (excluding one outlier, experiment 1c) gave the following fits:

300

301 B/Ca (mmol/mol) = .0604 (±0.0022) $[B(OH)_4^-]/[CO_3^{2-}]^{0.5}$ +.0411 (±0.012)   eq. 4

302

303 B/Ca (mmol/mol) = 2.88 (±0.13) [B]/[DIC] + 0.085 (±0.014)   eq. 5

304

305 where $[B(OH)_4^-]$, $[CO_3^{2-}]$, [B], and [DIC] are in units of μmol kg sw^{-1}, values in

306 parentheses are 1 standard error, all parameter estimates were significant ($p \leq 0.001$,

307 R^2=0.93 for eq. 4, R^2=0.89 for eq. 5).

308 Although our data provide no means of assessing whether B/Ca in the aragonite

309 precipitate depends upon solution $[B(OH)_4^-]/[CO_3^{2-}]^{0.5}$ or [B]/[DIC], the relationship

310 based on borate and carbonate was chosen for further investigation as CO_3^{2-} was

311 considered to be more relevant for precipitation than total DIC (see supplemental section

312 S6 for calculations based on DIC as well as Ca^{2+}).

313 Within any given experiment, the precipitate formed under a range of solution chemistry

314 conditions. However, the range within an experiment was generally small relative to the

315 differences among experiments. Thus K_D was assumed to be constant for a given

316 experiment allowing K_D values to be calculated for each individual experiment i:

317 $$\frac{B_i}{Ca_i} = \frac{B_i}{(CO_3)_i^{0.5}} = K_{D_i} \times \sum_{j=1}^{j=n} \frac{[B(OH)_4^-]_{i,j} \times w_{i,j}}{[CO_3^{2-}]_{i,j}^{0.5}}$$

318 Where B/Ca is measured and is in mmol/mol, $[B(OH)_4^-]$ and $[CO_3^{2-}]$ are in units of μmol

319 kg sw^{-1}, w is the fraction of total aragonite formed in time interval j as estimated from the

320 difference in expected and measured alkalinity, i signifies an individual experiment, and j

321 is one of n measurements taken during the course of aragonite precipitation in experiment

322   *i.* Aragonite is assumed to be pure $CaCO_3$, thus $Ca = CO_3$ with activities = 1, so the

323   exponent can be dropped for the solid phase. Calculated K_D values ranged from 0.042-

324   0.103, with an average of 0.071 +/- 0.011 sd. K_D values were correlated with a number

325   of solution chemistry parameters (Fig. S4), but regressions with [B] and either $[CO_3^{2-}]$ or

326   saturation state with respect to aragonite (Ω) explained much of the variance:

327

328   $K_D = -0.0109 (\pm 0.00157) [B] - 0.001106 (\pm 0.00021) \Omega + 0.0994 (\pm 0.00432)$ eq. 6

329

330   $K_D = -0.01215 (\pm 0.00159) [B] - 0.0000119 (\pm 0.000002) [CO_3^{2-}] + 0.09474 (\pm 0.00323)$

331   eq. 7

332   where [B] is in units of mmol kg sw^{-1}, and $[CO_3^{2-}]$ is in units of μmol kg sw^{-1}, with

333   $R^2=0.49$, $p<0.001$ and $R^2=0.53$, $p<0.001$ for equation 6 and 7 respectively. Note that

334   Ω and $[CO_3^{2-}]$ were highly correlated (Pearson correlation coefficient: 0.94).

335   Using eqs. 6-7, the B/Ca ratio for each precipitate was predicted based on each

336   measurement time-point. The differences between the measured and predicted B/Ca

337   ratios showed no significant correlation with any solution chemistry parameter (see

338   supplemental .xls file), nor was there any significant effect of temperature, calcein, nor of
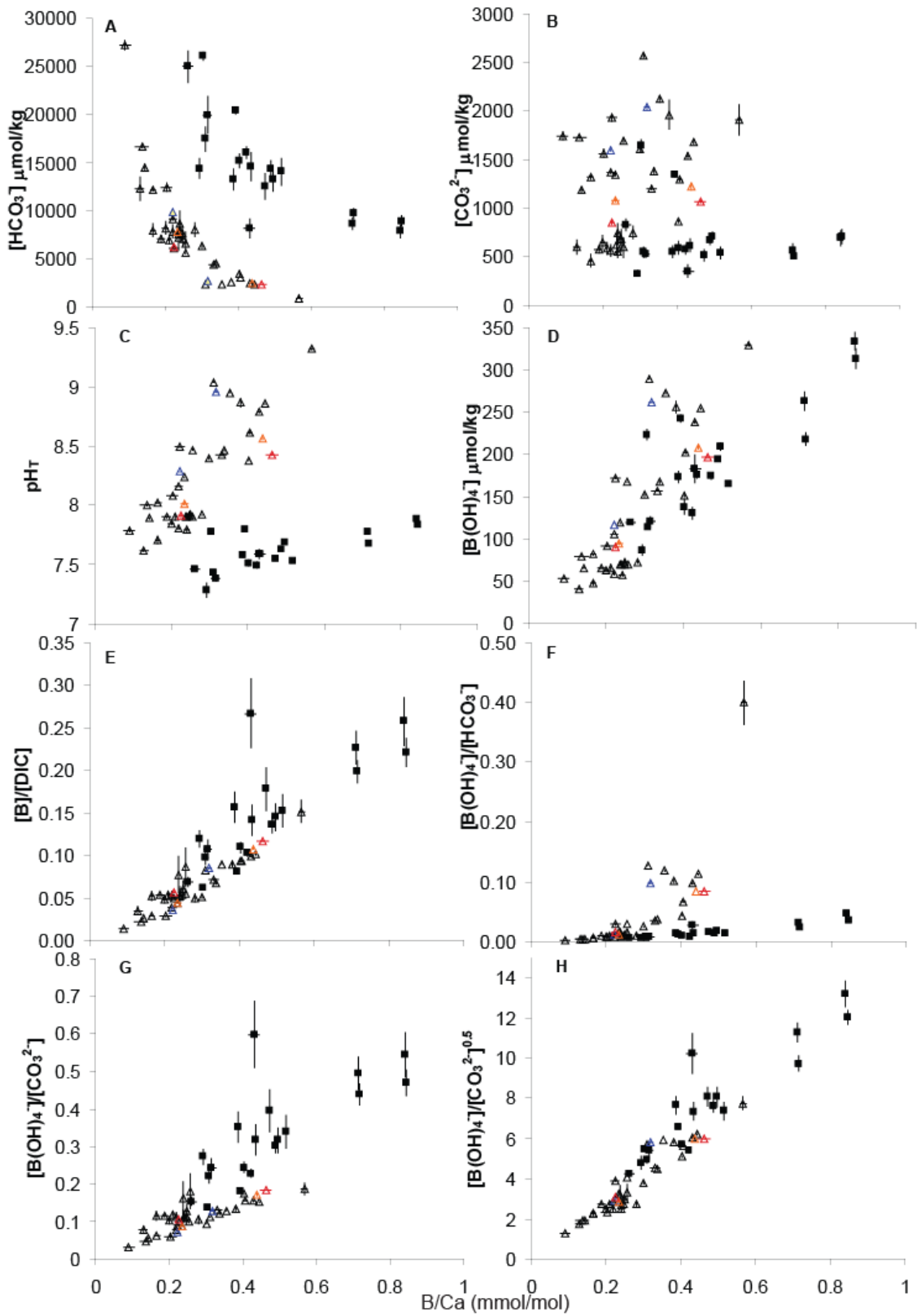
339   organic buffering compounds (though precipitates formed in the presence of HEPES

340   tended to have B/Ca ratios higher than predicted, while those formed in the presence of

341   TRIS tended to be lower). Differences between measured and predicted (for both

342   equations 6 and 7) B/Ca ratios were typically less than 0.03 mmol/mol or 8% relative

343   difference.

346   Figure 3. Relationship between B/Ca (mmol/mol) in aragonite and various solution

347   chemistry parameters. Units for all species in solution are μmol/kg sw. Symbols are as

348   described for figure 2.

349 *4. Discussion*

350 How boron is incorporated into aragonite remains uncertain. Many relationships (e.g.

351 Eqs. 1-3) have been proposed to explain how B/Ca depends on solution chemistry. The

352 wide range of solution chemistries achieved in our experiments allows us to evaluate

353 many of the proposed relationships.

354 In contrast to previous work (Hemming and Hanson, 1992), we found no significant

355 relationship between the B/Ca ratio in aragonite and the $[B(OH)_4^-]/[HCO_3^-]$ ratio in

356 solution (Fig. 3f). Rather, our results indicate that B/Ca depends on $[B(OH)_4^-]/[CO_3^{2-}]^{0.5}$

357 (Fig. 3h), suggesting that equation 2 represents the appropriate expression for the

358 distribution coefficient. A dependence of B/Ca on $[B(OH)_4^-]$ and $[CO_3^{2-}]$ is the most

359 likely scenario, due both to data suggesting $B(OH)_4^-$ to be the primary form of B

360 incorporated (e.g. Hemming et al., 1995; Mavromatis et al., 2015), and the involvement

361 of CO_3^{2-} in the formation of $CaCO_3$ (but see Wolthers et al., 2012). For a reaction

362 involving $B(OH)_4^-$ and CO_3^{2-}, a $B(OH)_4^-$ can balance the charge of only ½ a CO_3^{2-}, thus a

363 dependence on $[B(OH)_4^-]/[CO_3^{2-}]^{0.5}$ would be expected, consistent with our data (Fig.

364 3D).

365 Other possibilities do, however, exist. The significant correlation between B/Ca and

366 $[B(OH)_4^-]*[Ca^{2+}]$ could suggest the involvement of $CaB(OH_4)^+$, though it could also

367 reflect the importance of $[B(OH)_4^-]$ combined with a negative correlation between $[CO_3^{2-}$

368] and [Ca] in a sub-set of experiments (discussed further in the supplement). Variations in

369 [B]/[DIC] were strongly correlated with B/Ca and $[B(OH)_4^-]/[CO_3^{2-}]^{0.5}$ reflecting the

370 dependence of $[B(OH)_4^-]/[CO_3^{2-}]^{0.5}$ on [B] and [DIC] combined with the pH

371 dependencies of both B and DIC species; thus we cannot rule out the possibility of B/Ca

372   being controlled by [B]/[DIC]. For calcite, existing work points to [B]/[DIC] and growth

373   rate being the primary controls on B/Ca (Uchikawa et al., 2015). However, recalculating

374   the data of Uchikawa et al. (2015) as B/Ca / $[B(OH)_4^-]/[CO_3^{2-}]^{0.5}$ versus growth rate gives

375   a very similar fit to that obtained with [B]/[DIC] (R^2=0.86 vs 0.88), again reflecting the

376   difficulty of experimentally decoupling these parameters without simultaneously

377   changing other chemical parameters.

378

379   *4.1. Partition coefficient K_D*

380   Using our experimental data, we calculated partition coefficients (K_D) for $[B(OH)_4^-$

381   $]/[CO_3^{2-}]^{0.5}$ between aragonite and solution. This allows us to identify which factors

382   influence B/Ca ratios in addition to the primary control of the solution $[B(OH)_4^-]/[CO_3^{2-}$

383   $]^{0.5}$ ratio. The K_D appears to depend upon the boron concentration and the saturation state

384   or $[CO_3^{2-}]$ (equation 6, 7, Fig. S4). A dependence upon boron concentration is consistent

385   with previous work (Hemming et al., 1995), though our experiments likely did not cover

386   a large enough range of [B] to fully describe this dependence (discussed below). In

387   addition, we found a relationship between K_D and saturation state, which may reflect the

388   influence of growth rate because aragonite crystals precipitate faster from solutions of

389   greater supersaturation (e.g. Burton and Walter 1987). Other studies have also suggested

390   a growth rate influence on boron incorporation in calcite (Hobbs and Reardon, 1999;

391   Gabitov et al., 2014; Uchikawa et al., 2015) and aragonite (Mavromatis et al., 2015).

392   However, in contrast to the positive relationships between B/Ca and precipitation rate

393   observed previously, we found a negative, albeit weak, correlation between B/Ca and

394   precipitation rate (see supplemental .xls file for rates) or saturation state.

395   Several possibilities exist to explain the different signs of the effect of precipitation rate

396   on B/Ca between our experiments and previous studies. For studies on calcite, such

397   differences may reflect fundamental differences in how B is incorporated in calcite versus

398   aragonite (e.g. Kitano et al., 1978; Mavromatis et al., 2015), but such an explanation

399   cannot account for differences between our results and those of Mavromatis et al. (2015)

400   for aragonite. However, for experiments conducted at similar [B] to ours, B/Ca data of

401   Mavromatis et al., (2015) correlated with $[B(OH)_4^-]/[CO_3^{2-}]^{0.5}$ (calculated from Table 1 of

402   Mavromatis et al., (2015)) and when expressed as B/Ca / $[B(OH)_4^-]/[CO_3^{2-}]^{0.5}$ their K_D

403   values were consistently lower than those reported here (Table 2). The experiments of

404   Mavromatis et al. (2015) were conducted at lower saturation states than those used in our

405   study; thus such differences may reflect an effect of growth rate on B/Ca which is

406   particularly pronounced at low super-saturation states. It should also be noted that the

407   experiments of Mavromatis et al. (2015) were not conducted using seawater, so the ionic

408   composition of the fluid may influence partitioning (e.g. Kitano et al., 1978).

409

410   Alternatively, the expression used for the partition coefficient may play some role in the

411   observed correlations between B/Ca and precipitation rate.   Since K_D could be fit almost

412   equally well using saturation state (eq. 6) or $[CO_3^{2-}]$ (eq. 7), any dependence of K_D on Ω

413   may reflect the dependency of Ω on $[CO_3^{2-}]$. Thus the dependence of K_D on $[CO_3^{2-}]$ may

414   not reflect a growth rate effect associated with Ω, instead it could indicate that equation 2

415   does not fully describe the exchange reaction and that the relationship between $B(OH)_4^-$

416   and $[CO_3^{2-}]$ deviates from the 1 : 0.5 ratio used. Although a few of our experiments were

417   conducted at different $[CO_3^{2-}]$ but similar Ω, and vice-versa, and thus could potentially be

418   used to determine whether $[CO_3^{2-}]$ or Ω drives partitioning, no clear pattern was

419   observed.

420   Any influence of temperature or various additives was small relative to other sources of

421   variability as no significant effects were detected, which contrasts with some studies of

422   natural samples as well as one study of synthetic aragonite which point to a temperature

423   effect (Sinclair et al., 1998; Wara et al., 2003; Yu et al., 2007; Mavromatis et al., 2015).

424   It should be noted that because temperature influences saturation state, B and DIC

425   speciation, such effects, if not corrected for, could give rise to an apparent temperature

426   dependency for B/Ca. In the case of Mavromatis et al., (2015), the K_D expression used

427   was based on [B] and not $[B(OH)_4^-]$, thus changes in boron speciation with temperature

428   could account for the temperature influence; recalculating their data per equation 2

429   however shows no evidence for a temperature effect on K_D based on the same data

430   points.

431

432   *4.2. Prior K_D estimates*

433   Although the partitioning of B into aragonite has previously been investigated (Kitano et

434   al., 1978; Hemming et al., 1995; Mavromatis et al., 2015), only the study of Mavromatis

435   et al. (2015) characterized carbonate chemistry, thus making it difficult to compare our

436   results with much of the prior work. The experiments of Kitano et al. (1978) were similar

437   to our degassing experiments, but carbonate chemistry was not reported during

438   precipitation; given the range of carbonate chemistry values which can potentially be

439   generated during such an experiment we cannot satisfactorily estimate carbonate

440   chemistry for these experiments. Hemming and Hanson (1992) estimated K_D ~0.012 via

441 equation 1 (or 12 to be consistent with expressing B/Ca as mmol/mol as used elsewhere

442 in our paper) for biogenic calcium carbonate samples, which is well within the range

443 estimated in our study (Table 2). For the experiments of Hemming et al. (1995) detailed

444 carbonate chemistry measurements are lacking, however using their measured pH and

445 calculated $[Ca^{2+}]$, and our observation that precipitation typically starts near $\Omega = 20$, we

446 can make rough estimates of the relevant parameters: $[HCO_3^-] = 1000$ µmol/kg, $[CO_3^{2-}] =$

447 100 µmol/kg, and, depending upon the experiment, $[B(OH)_4^-] = 0.012, 0.107,$ or 0.78

448 mmol/kg. Using these values, we can estimate K_D via equation 1 and 2 (Table 2).

449 Despite experimental differences, the K_D estimates based on Hemming et al. (1995) fall

450 within the range of values found in the current study. Further, if we use equation 6 to

451 estimate K_D using the above constraints, we would predict a K_D range of 0.08 to 0.04,

452 and with equation 7: 0.09 to 0.05. At the boron concentration closest to seawater used by

453 Hemming et al. (1995), the difference between K_D predicted minus that calculated is -

454 0.001 for equation 6, and 0.01 for equation 7. The range of boron concentrations used by

455 Hemming et al. (1995) includes concentrations well below (~13% of seawater values)

456 those used in the current study, and at [B] well below seawater values, both equations 6

457 and 7 underestimate K_D. The study of Mavromatis et al. (2015) included boron

458 concentrations ranging from near seawater values to ~20x seawater values. At high [B],

459 both equation 6 and 7 predict negative K_D values for the Mavromatis et al. (2015) data,

460 indicating that neither equation can be reliably extrapolated far beyond the concentration

461 range used for fitting the equations. Within the range for which [B] was similar,

462 equations 6 and 7 both predicted K_D values higher (up to a factor of 10x) than those

463 calculated from Mavromatis et al. (2015). The highest Ω (5.8) used by Mavromatis et al.

464 (2015) was below the lowest values used in the current study, so a growth rate or

465 saturation state influence on K_D could be involved. Our experiment 1c, which

466 precipitated at a lower Ω than any of our other experiments had the lowest K_D, consistent

467 with a positive effect of growth rate at low Ω values.

468 The agreement between K_D estimates both across the diverse conditions used in the

469 current study and for independent studies, suggests that equations 6 and 7 provide

470 reasonable estimates of K_D over a wide range of conditions, except at [B]<<seawater,

471 [B]>>seawater, and Ω<~9.

472

473

474   Table 2. K_D values calculated using different equations for the current study and the

475   studies of Hemming et al. (1995) and Mavromatis et al. (2015). See discussion for

476   further details on the calculations. Note that K_D values expressed here are for expressing

477   B/Ca as mmol/mol. For the current study, mean values are expressed ± 1 standard

478   deviation.

Study	equation 1 K_D	equation 2 K_D
Hemming	4.5 (37 ppm B) -10 (0.59 ppm B)	0.04 (37 ppm B) - 0.1 (0.59 ppm B)
Mavromatis	0.3 – 40	0.0003 – 0.03
Current	1.4 – 52, mean 23 ± 14	0.042 - 0.103, mean 0.071 ± 0.011

479

480

481   *4.3. Nernst partition coefficient*

482   An alternative means of expressing partitioning is to use the single element or Nernst

483   partition coefficient (D_B), which is expressed as the ratio of the mass percent B in the

484   solid relative to the mass percent in solution (e.g. Gaetani and Cohen 2006). The use of

485   Nernst partition coefficients allows different studies to be compared as prior studies have

486   generally provided the necessary data. Values for Nernst partition coefficients are

487   dependent upon the specific experimental conditions (temperature, pH, competing

488   species, etc) (e.g. McIntire 1963), as they do not necessarily take into account speciation

489   changes or other factors influencing incorporation, thus comparisons should be

490   interpreted with this in mind. Values for D_B were calculated for each experiment as

491   described for K_D calculations, and are summarized in Table 3 along with those of other

492   studies. D_B values from the current study were strongly correlated with pH_T (pearson

493   correlation coefficient: 0.888), as well as with a wide range of other solution chemistry

494   parameters (Figure 4), likely reflecting changes in boron and carbon speciation with pH.

495   The following equations described much of the variance in D_B values:

496

497    $D_B = 8.215\ (\pm0.40)\ pH_T - 0.297\ (\pm0.035)\ \Omega - 55.69\ (\pm2.81)$ eq. 8

498    $D_B = 7.954\ (\pm0.378)\ pH_T - 0.267\ (\pm0.034)\ \Omega + 0.124\ (\pm0.038)\ T - 57.3\ (\pm2.6)$ eq. 9

499    $D_B = 7.429\ (\pm0.423)\ pH_T - 0.260\ (\pm0.033)\ \Omega + 0.114\ (\pm0.037)\ T - 0.491\ (\pm0.203)\ [B]\ -$

500    $52.5\ (\pm3.2)$ eq.10

501

502   Where Ω is the saturation state with respect to aragonite, pH_T is the pH on the total scale,

503   T is temperature in Celsius. All parameter estimates were significant at the $p<0.05$ level,

504   those for the constant, pH and saturation state were all highly significant ($p<0.001$), $R^2 =$

505   0.9, 0.92, and 0.93 for equation 8, 9, and 10 respectively. Note that D_B depends on

506   factors such as pH and temperature, whereas the K_D values did not, likely reflecting

507   changes in speciation of B and DIC as a function of pH and temperature which were

508   taken into account when calculating K_D.

509   Differences between the predicted (using equation 10) and measured solid composition

510   were not strongly correlated with any solution chemistry parameter, though there was a

511   weak positive correlation with growth rate and with salinity; no significant effects of

512   organic buffers were detected. Relative differences between measured and predicted

513   values were generally less than 16%.

514
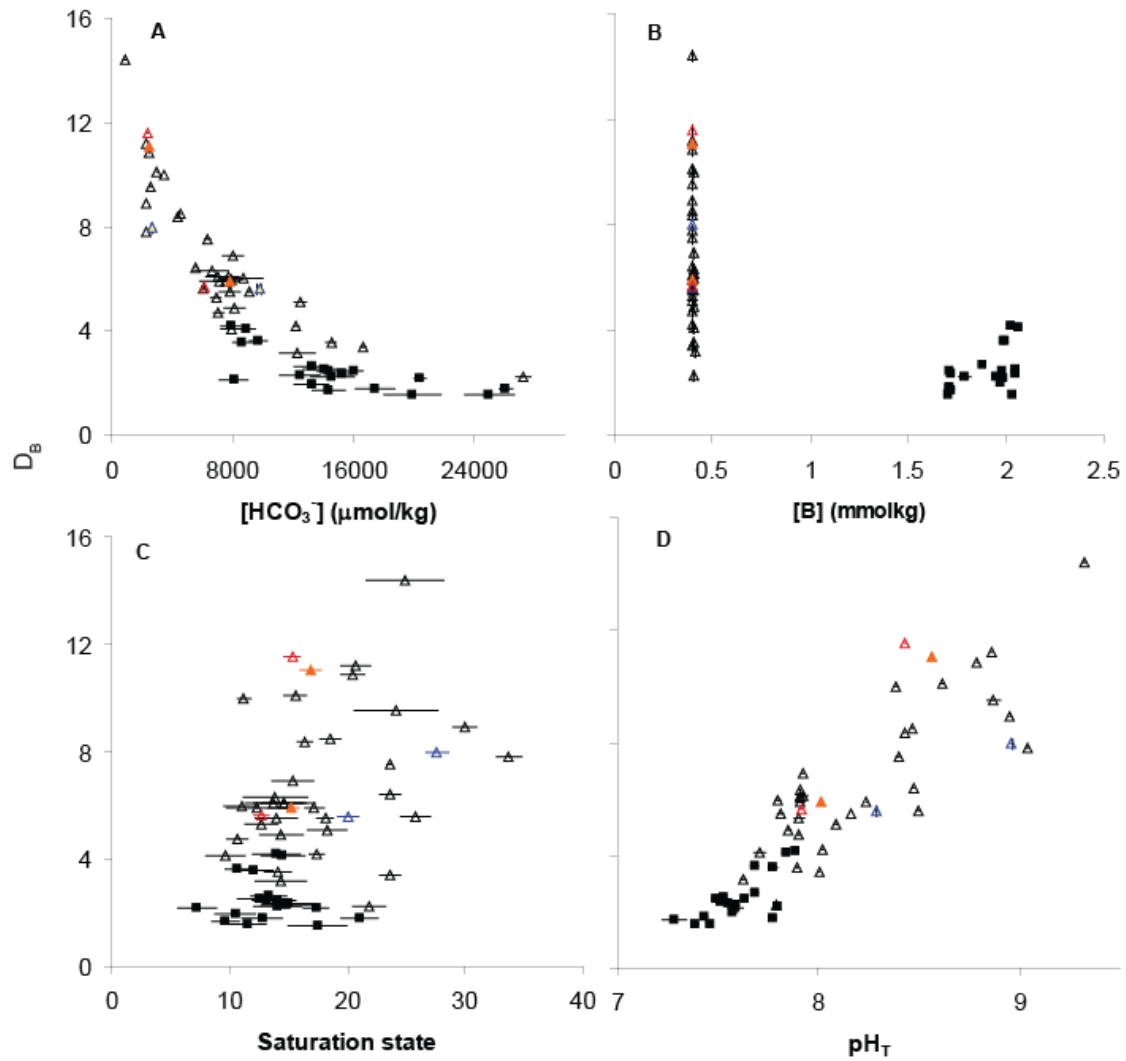
515

516   Figure 4. Relationship between the Nernst partition coefficient (D_B) and various solution

517   chemistry parameters. Symbols are as described for figure 2.

518

519   Table 3. Nernst coefficients (D_B) estimated from different studies. Note that for

520   estimating D_B for the Hemming and Hanson (1992) study, it was assumed that the

521   biogenic $CaCO_3$ samples precipitated from a solution with 4.676 ppm B, all other studies

522   represent synthetic aragonites and [B] was specified in the study.

Study	D_B
Kitano et al., 1978	~0.53 – 1.5
Hemming and Hanson, 1992	2-15
Hemming et al., 1995	10.2 – 22.8
Mavromatis et al., 2015	0.07 – 9
Current	1.5 – 14.4, mean 5.4 ± 3.0

523

524 Our estimates of D_B agree well with existing values – our experimental range covers the

525 range estimated for natural aragonite (Table 3). Our highest values overlap the lower

526 estimates of Hemming et al. (1995); for the two highest [B] used by Hemming et al., their

527 values are only slightly higher than some of our estimates at similar [B]. Estimates of D_B

528 from Kitano et al. (1978) and Mavromatis et al. (2015), though below those of Hemming

529 et al. (1995), also overlap our values, with their estimates for their lowest [B] being

530 similar to our values at similar [B]. Although both the D_B values of Kitano et al. (1978)

531 and Hemming et al. (1995) overlap ours, the values in the two studies do not overlap

532 (Table 3). This lack of agreement between these two previous studies likely reflects

533 differences in the carbonate chemistry during aragonite precipitation. In the experiments

534 performed by Hemming et al (1995), CO_2 diffusion into the solution controlled

535 precipitation, thus aragonite was formed under low [DIC] and low $[CO_3^{2-}]$ conditions,

536 with $[CO_3^{2-}]$ likely lower than any of our experiments or those of Kitano et al. (1978).

537 Such low $[CO_3^{2-}]$ conditions would in-turn lead to an increase in the $[B(OH)_4^-]/[CO_3^{2-}]^{0.5}$

538 ratio relative to other studies, thus a higher percentage of solution B would be expected to

539 be incorporated into the aragonite, consistent with high D_B estimates (Table 3). In

540 contrast, Kitano et al. (1978) used CO_2 degassing experiments, with much lower $[Ca^{2+}]$

541 and higher [DIC]. Although insufficient detail is given to estimate $[CO_3^{2-}]$ for these

542 experiments, concentrations were likely much higher than those of Hemming et al.

543 (1995), potentially similar to ours, consistent with similar D_B estimates. However,

544 Kitano et al. (1978) also used boron concentrations much higher than those used in the

545 current study, and high [B] resulted in lower D_B values.

546 The pattern of lower D_B or K_D values at higher [B] is consistent across studies.

547   Such observations have previously been suggested to be due to saturating defect sites at

548   which incorporation is more favorable at relatively low concentrations leaving only

549   structural sites for further substitution (Hemming et al., 1995). Changes in boron

550   speciation may also occur at high concentrations (e.g. Williams and Strack 1966) which

551   could further affect partitioning. It should also be noted that boron can influence the

552   growth of crystals along different axes (Ruiz-Agudo et al., 2012) and solution chemistry

553   influences surface charging which may further influence B incorporation (Hobbs and

554   Reardon 1999). Although our data provide insight into the controls on B incorporation

555   into aragonite in terms of bulk solution influences, there remains considerable research to

556   be done to understand the detailed mechanisms of B incorporation, particularly with

557   regards to the reactions and molecular rearrangements occurring near the crystal surface,

558   which ultimately control B incorporation and B/Ca ratios.

559

560   *4.4. Environmental proxies*

561   Although our results show patterns consistent with some studies of biologically formed

562   calcium carbonates e.g. $[B(OH)_4^-]/\Delta CO_3^{2-}$ was strongly correlated with B/Ca (Table 1;

563   Yu and Elderfield, 2007), such results cannot be directly compared. Here we directly

564   measure the chemistry during precipitation and thus correlate B/Ca in aragonite to the

565   chemistry in the solution from which that aragonite formed, whereas studies of material

566   in the natural environment usually measure seawater chemistry, not the chemistry of the

567   solution from which precipitation occurs, and thus make an assumption about the link

568   between seawater chemistry and the chemistry of the fluid responsible for precipitation.

569   Biologically formed aragonite is often formed from a solution substantially modified

570   from seawater, for instance, in corals aragonite growth occurs from a solution in which

571   pH and $[CO_3^{2-}]$ are elevated relative to the surrounding seawater (e.g. Al-Horani et al.,

572   2003; McCulloch et al., 2012; DeCarlo et al., 2015; Cai et al., 2016). Similarities in

573   relationships between B/Ca and seawater chemistry reported for biological samples and

574   relationships between B/Ca and directly measured solution chemistry in synthetic

575   precipitates suggests that variations in seawater chemistry affect the internal calcifying

576   environment of calcifying organisms. With the relationships described here for synthetic

577   aragonite, B/Ca holds potential as a proxy to determine how the chemistry of the internal

578   calcifying environment of biomineralizing organisms is linked to the external

579   environment. With this framework, B/Ca ratios of the shells and skeletons of calcifying

580   organisms can improve our understanding of how environmental conditions are recorded

581   in biogenic aragonite.

582

583

584   *5. Summary*

585   The B/Ca ratio in aragonite appears to be primarily a function of $[B(OH)_4^-]/[CO_3^{2-}]^{0.5}$ in

586   the solution from which aragonite growth occurs, with possible influences of [B] and

587   saturation state/$[CO_3^{2-}]$. For aragonites formed from seawater-like solutions, [B] can be

588   estimated from salinity, and since pH can be estimated from boron isotopes (e.g. Trotter

589   et al., 2011), $[B(OH)_4^-]$ can be calculated (assuming T is known), thus the remaining

590   variables influencing B/Ca are $[CO_3^{2-}]$ and potentially $[Ca^{2+}]$. B/Ca can be used to

591   estimate $[CO_3^{2-}]$, thus allowing the full carbonate chemistry under which the aragonite

592   formed to be estimated. If it can be shown that the solution chemistry from which

593 aragonite precipitates in a particular organism varies in a predictable way with seawater

594 chemistry, it may further be possible to use B/Ca in biogenic carbonates to infer past

595 seawater conditions.

596

611

612 **References**

613 **Al-Horani FA, Al-Moghrabi SM, de Beer D. 2003.** The mechanism of calcification and its

614   relation to photosynthesis and respiration in the scleractinian coral *Galaxea fascicularis*. Marine

615   Biol **142**: 419-426.

616 **Allen KA, Hönisch B, Eggins SM, Yu J, Spero HJ, Elderfield H. 2011**. Controls on boron

617   incorporation in cultured tests of the planktic foraminifer *Orbulina universa.* Earth and Planetary

618   Science Letters **309**:291-301 http://dx.doi.org/10.1016/j.epsl.2011.07.010.

619 **Allen KA, Hönisch B, Eggins SM, Rosenthal Y. 2012.** Environmental controls on B/Ca in

620   calcite tests of the tropical planktic foraminifer species Globigerinoides ruber and

621   Globigerinoides sacculifer. Earth and Planetary Science Letters **351–352**:270-280

622   http://dx.doi.org/10.1016/j.epsl.2012.07.004.

623   **Allison N, Cohen I, Finch AA, Erez J, Tudhope AW. 2014.** Corals concentrate dissolved

624   inorganic carbon to facilitate calcification. Nat Commun **5**10.1038/ncomms6741.

625   **Babila TL, Rosenthal Y, Conte MH. 2014.** Evaluation of the biogeochemical controls on B/Ca of

626   Globigerinoides ruber white from the Oceanic Flux Program, Bermuda. Earth and Planetary

627   Science Letters **404**:67-76 http://dx.doi.org/10.1016/j.epsl.2014.05.053.

628   **Burton EA, Walter LM. 1987.** Relative precipitation rates of aragonite and Mg calcite from

629   seawater: Temperature or carbonate ion control? Geology **15**: 111-114

630   **Cai W-J, Ma Y, Hopkinson BM, Grottoli AG, Warner ME, Ding Q, Hu X, Yuan X, Schoepf V,**

631   **Xu H, Han C, Melman T, Hoadley KD, Pettay DT, Matsui Y, Baumann JH, Levas S, Ying Y,**

632   **Wang Y. 2016.** Microelectrode characterization of coral daytime interior pH and carbonate

633   chemistry. Nature Communications **7**:11144

634   **Culberson C, Pytkowicz RM. 1968.** Effect of pressure on carbonic acid, boric acid, and the pH

635   in seawater. Limnology and Oceanography **13**:403-417

636   **DeCarlo TM, Gaetani GA, Holcomb M, Cohen AL. 2015.** Experimental determination of factors

637   controlling U/Ca of aragonite precipitated from seawater: Implications for interpreting coral

638   skeleton. Geochimica et Cosmochimica Acta **162**:151-165

639   http://dx.doi.org/10.1016/j.gca.2015.04.016.

640   **de Nooijer LJ, Spero HJ, Erez J, Bijma J, Reichart GJ. 2014.** Biomineralization in perforate

641   foraminifera. Earth-Science Reviews **135**:48-58

642   http://dx.doi.org/10.1016/j.earscirev.2014.03.013.

643   **Dickson AG. 1990.** Thermodynamics of the dissociation of boric acid in synthetic seawater from

644   273.15 to 318.15 K. Deep-Sea Research **37**:755-766

645   **Dissard D, G. Nehrke, G. J. Reichart, J. Nouet, and J. Bijma. 2009.** Effect of the fluorescent

646   indicator calcein on Mg and Sr incorporation into foraminiferal calcite. Geochem Geophys

647   Geosyst **10**:Q11001 doi:10.1029/2009GC002417.

648   **Douville E, Paterne M, Cabioch G, Louvat P, Gaillardet J, Juillet-Leclerc A, Ayliffe L. 2010.**

649   Abrupt sea surface pH change at the end of the Younger Dryas in the central sub-equatorial

650   Pacific inferred from boron isotope abundance in corals (*Porites*). Biogeosciences

651   **7**:2445-2459 10.5194/bg-7-2445-2010.

652   **Foster GL. 2008.** Seawater pH, pCO2 and [CO2−3] variations in the Caribbean Sea over the last

653   130 kyr: A boron isotope and B/Ca study of planktic foraminifera. Earth and Planetary Science

654   Letters **271**:254-266 10.1016/j.epsl.2008.04.015.

655   **Gabitov RI, Schmitt AK, Rosner M, McKeegan KD, Gaetani GA, Cohen AL, Watson EB,**

656   **Harrison TM. 2011.** In situδ7Li, Li/Ca, and Mg/Ca analyses of synthetic aragonites.

657   Geochemistry Geophysics Geosystems **12**10.1029/2010gc003322.

658   **Gabitov RI, Rollion-Bard C, Tripati A, Sadekov A. 2014.** In situ study of boron partitioning

659   between calcite and fluid at different crystal growth rates. Geochimica et Cosmochimica Acta

660   **137**:81-92 10.1016/j.gca.2014.04.014.

661   **Gaetani GA, Cohen AL. 2006.** Element partitioning during precipitation of aragonite from

662   seawater: a framework for understanding paleoproxies. Geochimica et Cosmochimica Acta

663   **70**:4617-4634

664   **Hain MP, Sigman DM, Higgins JA, Haug GH. 2015.** The effects of secular calcium and

665   magnesium concentration changes on the thermodynamics of seawater acid/base chemistry:

666   Implications for Eocene and Cretaceous ocean carbon chemistry and buffering. Global

667   Biogeochemical Cycles **29**:2014GB004986 10.1002/2014gb004986.

668   **Hathorne EC, Gagnon A, Felis T, Adkins J, Asami R, Boer W, Caillon N, Case D, Cobb KM,**

669   **Douville E, deMenocal P, Eisenhauer A, Garbe-Schönberg CD, Geibert W, Goldstein S,**

670   **Hughen K, Inoue M, Kawahata H, Kölling M, Le Cornec F, Linsley BK, McGregor HV,**

671   **Montagna P, Nurhati IS, Quinn TM, Raddatz J, Rebaubier H, Robinson L, Sadekov A,**

672   **Sherrell R, Sinclair D, Tudhope AW, Wei G, Wong H, Wu HC, You C-F. 2013.** Inter-

673   laboratory study for coral Sr/Ca and other element/Ca ratio measurements.Geochemistry,

674   Geophysics, Geosystems:n/a-n/a 10.1002/ggge.20230.

675   **He M, Xiao Y, Jin Z, Liu W, Ma Y, Zhang Y, Luo C. 2013.** Quantification of boron incorporation

676   into synthetic calcite under controlled pH and temperature conditions using a differential

677   solubility technique. Chemical Geology **337–338**:67-74

678   http://dx.doi.org/10.1016/j.chemgeo.2012.11.013.

679   **Hemming NG, Hanson GN. 1992.** Boron isotopic composition and concentration in modern

680   marine carbonates. Geochimica et Cosmochimica Acta **56**:537-543

681   http://dx.doi.org/10.1016/0016-7037(92)90151-8.

682   **Hemming NG, Reeder RJ, Hanson GN. 1995.** Mineral-fluid partitioning and isotopic fractionation

683   of boron in synthetic calcium carbonate. Geochimica et Cosmochimica Acta **59**:371-379

684   http://dx.doi.org/10.1016/0016-7037(95)00288-B.

685   **Henehan MJ, Rae JWB, Foster GL, Erez J, Prentice KC, Kucera M, Bostock HC, Martínez-**

686   **Botí MA, Milton JA, Wilson PA, Marshall BJ, Elliott T. 2013.** Calibration of the boron isotope

687   proxy in the planktonic foraminifera *Globigerinoides ruber* for use in palaeo-CO_2 reconstruction.

688   Earth and Planetary Science Letters **364**:111-122 10.1016/j.epsl.2012.12.029.

689   **Henehan MJ, Foster GL, Rae JWB, Prentice KC, Erez J, Bostock HC, Marshall BJ, Wilson**

690   **PA. 2015.** Evaluating the utility of B/Ca ratios in planktic foraminifera as a proxy for the

691   carbonate system: A case study of Globigerinoides ruber. Geochemistry, Geophysics,

692   Geosystems **16**:1052-1069 10.1002/2014gc005514.

693   **Hobbs MY, Reardon EJ. 1999.** Effect of pH on boron coprecipitation by calcite: Further evidence

694   for nonequilibrium partitioning of trace elements. Geochimica et Cosmochimica Acta **63**:1013-

695   1021

696   **Holcomb M, Cohen AL, Gabitov RI, Hutter JL. 2009.** Compositional and morphological features

697   of aragonite precipitated experimentally from seawater and biogenically by corals. Geochimica

698   et Cosmochimica Acta **73**:4166-4179 10.1016/j.gca.2009.04.015.

699   **Kaczmarek K, Langer G, Nehrke G, Horn I, Misra S, Janse M, Bijma J. 2015.** Boron

700   incorporation in the foraminifer Amphistegina lessonii under a decoupled carbonate chemistry.

701   Biogeosciences **12**:1753-1763 10.5194/bg-12-1753-2015.

702   **Kinsman DJJ, Holland HD. 1969.** The co-precipitation of cations with CaCO3 - IV. The co-

703   precipitation of Sr2+ with aragonite between 16 and 96 C. Geochimica et Cosmochimica Acta

704   **33**: 1-17

705   **Kitano Y, Okumura M, Idogaki M. 1978.** Coprecipitation of borate-boron with calcium carbonate.

706   Geochemical Journal **12**:183 - 189

707   **Klochko K, Cody GD, Tossell JA, Dera P, Kaufman AJ. 2009.** Re-evaluating boron speciation

708   in biogenic calcite and aragonite using 11B MAS NMR. Geochimica et Cosmochimica Acta

709   **73**:1890-1900 10.1016/j.gca.2009.01.002.

710   **Klochko K, Kaufman AJ, Yao W, Byrne RH, Tossell JA. 2006.** Experimental measurement of

711   boron isotope fractionation in seawater. Earth and Planetary Science Letters **248**:276-285

712   10.1016/j.epsl.2006.05.034.

713   **Mass T, Drake JL, Haramaty L, Kim JD, Zelzion E, Bhattacharya D, Falkowski PG. 2013.**

714   Cloning and characterization of four novel coral acid-rich proteins that precipitate carbonates in

715   vitro. Current Biology **23**:1126-1131 10.1016/j.cub.2013.05.007.

716   **Mavromatis V, Montouillout V, Noireaux J, Gaillardet J, Schott J. 2015**. Characterization of

717   boron incorporation and speciation in calcite and aragonite from co-precipitation experiments

718   under controlled pH, temperature and precipitation rate. Geochimica et Cosmochimica Acta

719   150: 299-313

720   **McCulloch M, Falter J, Trotter J, Montagna P. 2012.** Coral resilience to ocean acidification and

721   global warming through pH up-regulation. Nature Clim Change **2**:623-627

722   **McIntire WL. 1963.** Trace element partition coefficients - a review of theory and applications to

723   geology. Geochimica et Cosmochimica Acta **27**:1209-1264

724   **Ni Y, Foster GL, Bailey T, Elliott T, Schmidt DN, Pearson P, Haley B, Coath C. 2007.** A core

725   top assessment of proxies for the ocean carbonate system in surface-dwelling foraminifers.

726   Paleoceanography **22**:n/a-n/a 10.1029/2006pa001337.

727   **Pearson PN, Palmer MR. 1999.** Middle Eocene Seawater pH and Atmospheric Carbon Dioxide

728   Concentrations. Science **284**:1824-1826 10.1126/science.284.5421.1824.

729   **Pelejero C, Calvo E, McCulloch MT, Marshall JF, Gagan MK, Lough JM, Opdyke BN. 2005.**

730   Preindustrial to Modern Interdecadal Variability in Coral Reef pH. Science **309**:2204-2207

731   **Penman DE, Hönisch B, Rasbury ET, Hemming NG, Spero HJ. 2013.** Boron, carbon, and

732   oxygen isotopic composition of brachiopod shells: Intra-shell variability, controls, and potential

733   as a paleo-pH recorder. Chemical Geology **340**:32-39 10.1016/j.chemgeo.2012.11.016.

734   **Rae JWB, Foster GL, Schmidt DN, Elliott T. 2011.** Boron isotopes and B/Ca in benthic

735   foraminifera: Proxies for the deep ocean carbonate system. Earth and Planetary Science

736   Letters **302**:403-413 10.1016/j.epsl.2010.12.034.

737   **Rollion-Bard C, Blamart D, Trebosc J, Tricot G, Mussi A, Cuif J-P. 2011.** Boron isotopes as

738   pH proxy: A new look at boron speciation in deep-sea corals using 11B MAS NMR and EELS.

739   Geochimica et Cosmochimica Acta **75**:1003-1012 10.1016/j.gca.2010.11.023.

740   **Ruiz-Agudo E, Putnis CV, Kowacz M, Ortega-Huertas M, Putnis A. 2012.** Boron incorporation

741   into calcite during growth: Implications for the use of boron in carbonates as a pH proxy. Earth

742   and Planetary Science Letters **345-348**:9-17 10.1016/j.epsl.2012.06.032.

743   **Sanyal A, Hemming NG, Broecker WS, Lea DW, Spero HJ, Hanson GN. 1996.** Oceanic pH

744   control on the boron isotopic composition of foraminifera: Evidence from culture experiments.

745   Paleoceanography **11**:513-517 10.1029/96pa01858.

746   **Sanyal A, Nugent M, Reeder RJ, Bigma J. 2000.** Seawater pH control on the boron isotopic

747   composition of calcite: evidence from inorganic calcite precipitation experiments. Geochimica et

748   Cosmochimica Acta **64**: 1551-1555

749   **Sen S, Stebbins JF, Hemming NG, Ghosh B. 1994.** Coordination environments of B impurities

750   in calcite and aragonite polymorphs: A 11B MAS NMR study. American Mineralogist **79**:819-

751   825

752   **Sinclair DJ, Kinsley LPJ, McCulloch MT. 1998.** High resolution analysis of trace elements in

753   corals by laser ablation ICP-MS. Geochimica et Cosmochimica Acta **62**: 1889-1901

754   **Tripati AK, Roberts CD, Eagle RA, Li G. 2011.** A 20 million year record of planktic foraminiferal

755   B/Ca ratios: Systematics and uncertainties in pCO2 reconstructions. Geochimica et

756   Cosmochimica Acta **75**:2582-2610 http://dx.doi.org/10.1016/j.gca.2011.01.018.

757   **Trotter J, Montagna P, McCulloch M, Silenzi S, Reynaud S, Mortimer G, Martin S, Ferrier-**

758   **Pagès C, Gattuso J-P, Rodolfo-Metalpa R. 2011.** Quantifying the pH 'vital effect' in the

759   temperate zooxanthellate coral Cladocora caespitosa: Validation of the boron seawater pH

760   proxy. Earth and Planetary Science Letters **303**:163-173 10.1016/j.epsl.2011.01.030.

761   **Uchikawa J, Penman DE, Zachos JC, Zeebe RE. 2015.** Experimental evidence for kinetic

762   effects on B/Ca in synthetic calcite: Implications for potential B(OH)4– and B(OH)3

763   incorporation. Geochimica et Cosmochimica Acta **150**:171-191 10.1016/j.gca.2014.11.022.

764   **van Heuven S, Pierrot D, Lewis E,Wallace DWR. 2009.** MATLAB Program developed for CO2

765   system calculations. ORNL/CDIAC-105b. Carbon Dioxide Information Analysis Center, Oak

766   Ridge National Laboratory, U.S. Department of Energy, Oak Ridge, TN.

767   **Venn AA, Tambutte E, Holcomb M, Laurent J, Allemand D, Tambutte S. 2013.** Impact of

768   seawater acidification on pH at the tissue-skeleton interface and calcification in reef corals.

769   Proc Natl Acad Sci U S A **110**:1634-1639 10.1073/pnas.1216153110.

770   **Wang Z, Hu P, Gaetani G, Liu C, Saenger C, Cohen A, Hart S. 2013.** Experimental calibration

771   of Mg isotope fractionation between aragonite and seawater. Geochimica et Cosmochimica

772   Acta **102**:113-123 10.1016/j.gca.2012.10.022.

773   **Wara MW, Delaney ML, Bullen TD, Ravelo AC. 2003.** Possible roles of pH, temperature, and

774   partial dissolution in determining boron concentration and isotopic composition in planktonic

775   foraminifera. Paleoceanography **18**:n/a-n/a 10.1029/2002pa000797.

776   **Williams PM, Strack PM. 1966.** Complexes of boric acid with organic cis-diols in seawater.

777   Limnology and Oceanography **11**:401-404

778   **Wolthers M, Nehrke G, Gustafsson JP, Van Cappellen P. 2012.** Calcite growth kinetics:

779   Modeling the effect of solution stoichiometry. Geochimica et Cosmochimica Acta **77**:121-134

780   http://dx.doi.org/10.1016/j.gca.2011.11.003.

781   **Xiao Y, Li H, Liu W, Wang X, Jiang S. 2008.** Boron isotopic fractionation in laboratory inorganic

782   carbonate precipitation: evidence for the incorporation of B(OH)3 into carbonate. Science in

783   China Series D: Earth Sciences **51**:1776-1785 10.1007/s11430-008-0144-y.

784   **Yu J, Elderfield H. 2007.** Benthic foraminiferal B/Ca ratios reflect deep water carbonate

785   saturation state. Earth and Planetary Science Letters **258**:73-86 10.1016/j.epsl.2007.03.025.

786   **Yu J, Elderfield H, Hönisch B. 2007.** B/Ca in planktonic foraminifera as a proxy for surface

787   seawater pH. Paleoceanography **22**:n/a-n/a 10.1029/2006pa001347.

788

789

790

791 **Supplemental materials**

792 Detailed methods and associated discussion, figures, and tables

793

794 *S1. Precipitation details*

795 *S1.1. Reagents*

796 Seawater drawn continuously from ~4 m depth, ~200 m off-shore in Vineyard Sound

797 (Massachusetts, USA), passed through a sand filter and distributed throughout the

798 Environmental Systems Laboratory (WHOI) was used for all experiments. The seawater

799 used for experiments was further passed through pleated Flow Max cartridge filters (final

800 size 0.35 µm), and finally a 0.2 µm Whatman Polycap 36tc filter (lot y830) and stored in

801 HDPE carboys (all filters and carboys were rinsed repeatedly prior to collecting

802 seawater). Seawater was collected on three different dates in 2011 and 2013 and stored

803 in the dark for no more than 6 weeks prior to use in experiments.

804 Concentrated seawater (2xsw) was prepared by placing seawater in pre-washed ~1 L

805 polypropylene (PP) containers (MicroLite, Anchor Packaging) held within warm water

806 baths (50 – 70 $^{\circ}$C) and allowing it to evaporate until the mass halved. 2xsw used in 2011

807 was not filtered, while that used in 2013 was passed through a 0.45 µm filter (Millipore

808 HAWP) prior to use.

809 Calcium carbonate was from Alfa Aesar (puratronic stock 43073 lot l16Q78 - used for

810 runs in 2011 and degassing runs 1-4 in 2013, or stock 10996 lot C24U037 for runs 5 - 7

811 in 2013 as well as the fsw containing $CaCO_3$ used in pumping runs 13g and 8f).

812 Strontium carbonate was from Alfa Aesar (puratronic stock 36618, lot 23557 used in

813 2011, lot 23399 in 2013), as was sodium carbonate (puratronic stock 10861 lot 23390 or

814   23776). Other reagents were obtained from various suppliers: $NaHCO_3$ (Acros

815   424270010 lot a0200805001 for 2011 and 13g, 10h, 6c, and 7d in 2013; Alfa Aesar stock

816   10863 lot S70421 for other 2013 experiments), calcein (Alfa Aesar L10255 lot

817   10132899), OTC (oxytetracycline dihydrate, Acros 123840100 lot A0275864), TRIS

818   base (Fisher t395 lot 064221 used in 2011, or lot 104689 used in 2013), $Na_2B_4O_7\ 10H_2O$

819   (Baker 3568 lot C13634), NaOH (Fisher s318 lot 975017), HEPES sodium salt (Fisher

820   BP2939 lot 107739), $CaCl_2$ (Alfa Aesar 10043-52-4, stock L13191 lot 10113722), $MgCl_2$

821   (Alfa Aesar stock 12315 lot f18w011).

822   Water used for preparing solutions and cleaning was either quartz distilled (used in 2011)

823   or filtered (18 MΩ, Barnstead Nanopure; used in 2013).

824

825   *S.1.2. Aragonite growth set-up*

826   All experiments conducted in 2011 used ~1 L PET containers (Deli Gourmet, Solo) for

827   aragonite growth, while in 2013 ~1 L PP containers (MicroLite, Anchor Packaging) were

828   used for most experiments. The choice of container has little impact on the experiment

829   (unpublished data). Precipitates grown in PET containers were generally easier to

830   recover than those grown in PP containers, but, PET tends to be damaged by acid

831   washing, thus when precipitates were to be used primarily for trace element composition

832   and thus all glass and plastic ware acid (HCl) washed prior to use, PP containers were

833   used.

834

835   Some experiments were bubbled with air, CO_2, or mixtures there-of. Air/CO_2 mixtures

836   were prepared using mass flow controllers. The pCO_2 of both the mixed gasses and air

837   was determined using a NDIR CO_2 analyzer (Qubit S-151). Atmospheric pressure in the

838   lab was recorded (dial barometer, Fisher) each time the gas composition was measured –

839   values were generally near 770 mmHg. Gas flows to individual experiments were

840   controlled with rotameters. All gasses were bubbled through de-ionized water prior to

841   being introduced into experimental containers to humidify the air and thus reduce

842   evaporation of the experimental solution. Gasses were introduced into a given

843   experiment via a glass tube with a glass frit to diffuse the air near the bottom of each

844   experimental container.

845

846   For pumping experiments, glass and teflon syringes (SGE gastight) were used to add

847   reagents in 2011, polypropylene/polyethylene syringes (Norm-ject, Henke-Sass Wolf) in

848   2013. Vinyl tubing (Cole-Parmer 30526-18) was used to carry reagents from the syringe

849   to the experimental container. Syringes and tubing were washed with dilute HCl, H_2O,

850   and the given reagent prior to use.

851   Details specific to individual experiments are provided in Table S1.

852

853   *S1.3. Weights*

854   All solutions added to or removed from an experiment were weighed using an Ohaus

855   precision standard model ts4kd balance, the calibration was verified using reference

856   masses prior to each group of experiments (measured reference values were within 0.03%

857   of expected). Most reagents and all dilutions of alkalinity samples were weighed to four

858   or five decimal places (Sartorius cpa124s or bp211d balances); reference weights were

859   within 0.006% of expected values.

860

S1.4. Stirring

All solutions were stirred continuously during precipitation. This was affected using one

of three different methods. An overhead stirrer set at 120 rpm was used to rotate a PTFE

impeller with 4 angled blades (~4 cm diameter) for all 2013 experiments ending "g" or

"h" and 2011 experiments ending "1" or "2". Experiments ending a-f were stirred with

PTFE coated octagonal magnetic stir bars ~5.1 cm long and 0.8 cm diameter at a rate of

130 rpm. In 2011, stir bars were placed directly on the bottom of the containers. To

reduce problems with the stir bar grinding the growing precipitates, stir bars were

suspended ~2 cm from the bottom of the container using nylon monofilament line for

experiments conducted in 2013. The line was attached to a swivel, thus the stir bar could

rotate freely.

S2. Solution chemistry and calculations

S2.1. Salinity

The final salinity as well as the initial salinity of seawater based reagents was

measured using a conductivity probe (Hach). Conductivity values were converted to

salinity using equations of Fofonoff (1985). The initial seawater and a sub-set of final

solutions were also measured using a Guildline autosal model 8400B salinometer.

IAPSO standard seawater (batch P-153) was used to standardize the autosal before runs.

For samples measured using both methods, agreement was generally within 0.5, though

values measured using the Hach conductivity probe were invariably offset from the

882   autosal values, thus a correction was applied to the values measured using the Hach probe

883   to better match the autosal values.

884

885   *S2.2. Alkalinity and pH*

886   Alkalinity measurements were carried out per Holcomb et al. (2012), most samples were

887   diluted with a ~39 g NaCl/L solution at the time of collection to prevent precipitation

888   prior to measurement and to reduce the alkalinity to <5200 µmol alkalinity/kg sw. When

889   appropriate, the calculations were corrected for the presence of added buffers. Due to the

890   experimental solutions departing from seawater composition, a number of modifications

891   were made to otherwise standard calculations – see section S2.3.

892   All pH measurements (recorded to 0.1 mV) were made on unfiltered samples using an

893   Orion Ross 8165 pH electrode and an Orion 3-star meter calibrated against NBS buffers

894   (Ricca). Solutions for pH measurement were placed in a tube in a temperature controlled

895   bath (~ 25 $^{\circ}$C) and stirred during pH measurement. Periodic measurements of either

896   certified seawater reference material (CRM-107 or 117, supplied by Andrew Dickson,

897   Scripps Institute of Oceanography) or an in-house standard were made to estimate the

898   offset between pH_{NBS} and pH_T. The pH_T for the standard seawater solutions was

899   calculated based on TA and DIC using CO2Sys (van Heuven et al., 2009) with constants

900   from Mehrbach et al. (1973) as refit by Dickson and Millero (1987), and Dickson (1990)

901   for sulfate. Measurements were then corrected to the total scale assuming that drift in the

902   offset value was linear with time between times at which it was determined.

903   Occasionally values for alkalinity or pH were not obtained at a given measurement time-

904   point. When this occurred, values were interpolated based on measurements made before

905   and after the missing value and calculated rates of alkalinity depletion – the rate of

906   alkalinity depletion was assumed to remain stable over the period affected by a missing

907   alkalinity value.

908

909

910   *S2.3. Salinity corrections*

911   Due to the addition of different compounds to seawater, standard seawater salinity to

912   composition and ion activity relationships do not apply to most time-points in our

913   experiments. For example, addition of $MgCl_2$ adds conductivity (and thus changes

914   salinity) and affects ion activities, yet makes no contribution to alkalinity, nor does it

915   contribute other species which usually vary in direct proportion to salinity. A number of

916   calculations (titration alkalinity, carbonate chemistry parameters, etc.) make use of

917   salinity to composition relationships to simplify calculations. To compensate for

918   compositional differences, a number of modifications were made to these otherwise

919   standard calculations.

920

921   *S2.3.1. Titration alkalinity corrections*

922   For the calculation of titration alkalinity, a regression analysis was used (Holcomb et al.,

923   2012). This code uses salinity to concentration relationships to calculate concentrations

924   of B, F, etc., as well as salinity dependencies for estimating carbonate equilibrium

925   constants. The concentrations of NH_4, H_2SiO_4, and PO_4 were assumed to be 0 in all

926   solutions, and all reagents used were assumed to be free from compounds that would

927   affect alkalinity calculations except for those specifically considered. TRIS, HEPES, and

928   boron were added to certain experiments. The contribution of boron is normally

929   considered in calculating alkalinity, so only the B concentration was adjusted to account

930   for the added B. To account for the contribution of TRIS we used a pKa value calculated

931   from equation 27 of Dickson (1993). For HEPES, we are unaware of reported pKa

932   values for seawater media, thus a pKa of 7.5 was assumed. Since most alkalinity samples

933   were diluted with a NaCl solution (~39 g NaCl/L – with an assumed salinity of 32 and no

934   contribution to alkalinity), concentrations of different species (B, F, etc.) and salinities

935   were corrected for sample dilution. Due to the addition of various reagents over the

936   course of each experiment, the measured final salinities (calculated from conductivity) do

937   not reflect seawater composition, nor do they capture the evolution of solution chemistry

938   over time. However, for most pumping experiments, the error introduced by ignoring

939   such salinity changes is less than 1 μmol alkalinity/kg sw, whereas the typical relative

940   standard deviation for repeated alkalinity measurements is 0.2%, or ±5 μmol alkalinity/kg

941   sw at a typical seawater alkalinity, thus no attempt was made to further correct salinity,

942   and the final measured salinity was used for calculations. For degassing experiments

943   there was a greater difference between measured salinity and that of seawater (due to the

944   addition of $MgCl_2$), thus a salinity of 32.5 was used for calculating the concentrations of

945   different species in the experimental fluid, while the measured final salinity was used for

946   calculating equilibrium constants. All NaX solutions were assumed to have a salinity of

947   0 for calculating concentrations of species contributing to alkalinity, and S = 4.5 for

948   calculating equilibrium constants – though due to samples being substantially diluted

949   with the NaCl solution prior to measurement, the final salinity used for calculating

950   constants was invariably near 32.

951

S2.3.2. Carbonate chemistry corrections

Calculations of the full carbonate system chemistry and concentrations of different

species are more sensitive to errors in salinity estimates than titration alkalinity

calculations, thus a more rigorous set of corrections were used for these calculations.

Two different salinity values were used for calculations. The empirical equilibrium

constants used for calculating inorganic carbon, boron, etc. speciation are functions of

salinity (reflecting the influence of ionic strength on ion activities). Thus the addition of

ions (such as contributed by NaX solutions, or $MgCl_2$) affects salinity, ionic strength, and

in-turn, equilibrium constants. Although the influence of the ions added in this

experiment on equilibrium constants likely differs from that expected based purely on

changes in salinity (estimated from conductivity), we assumed that the compositional

changes were sufficiently small that seawater derived salinity relationships could still be

used for calculating equilibrium constants. For estimating concentrations of species such

as B, F, SO_4, Ca, etc., the measured salinity values could not be used due to ions added

with the NaX or $MgCl_2$ solutions contributing to salinity but not affecting concentrations

of other species present in seawater. Thus, measured salinities were corrected for the

contribution of the added ions. The ionic equivalent conductivities reported by

Pawlowicz (2010) were used to estimate the contribution of the added NaX or $MgCl_2$ to

conductivity, and equations from Fofonoff (1985) to convert conductivity to salinity.

Due to differences in how different experiments were conducted, slightly different

procedures were used for calculating salinity at different time-points.

973

974   For degassing experiments, the initial salinity of the solution was unknown due to

975   evaporation potentially occurring during the dissolution of reagents with CO_2. The final

976   measured salinity was however known. Since the degassing experiments used a modified

977   seawater solution in which the primary salt added was $MgCl_2$, the salinity values used for

978   calculating concentrations were corrected for the presence of $MgCl_2$ by subtracting the

979     $MgCl_2$ contribution from the total salinity. To compensate for evaporation, the

980   evaporation rate was estimated from the difference in expected and measured final

981   solution mass relative to the total time for each experiment. For each group of

982   experiments (run simultaneously from the same starting solution), the median

983   evaporation rate was used to correct the salinity for each time point. Most experiments

984   from a given group were run for a similar length of time and had similar evaporation rates

985   (typically 0.5 to 2 g/day, depending upon the set of experiments; excluding suspect

986   values, the range within a group was less than 0.7 g/day), but one experiment departed

987   from this pattern (we suspect the final weight recorded was incorrect). By using the

988   median evaporation rate for each group of experiments we were able to avoid one

989   potentially erroneous value influencing the interpretation. Precipitation of $CaCO_3$ was

990   not included in correcting salinity values as it had relatively little impact.

991

992   For pumping experiments, the salinity of the initial seawater was known, thus the

993   expected salinity at any point in time could be calculated based on the initial salinity and

994   the salinity of solutions added to the experiment. The 2xsw solution was assumed to

995   have a salinity of 64, which contributed both to the salinity value used to calculate

996   constants and to that used for concentrations. The sw solution containing $CaCO_3$ and

997    $SrCO_3$ added in two of the pumping experiments was assumed to have S = 31.9. The

998   NaX solutions were assumed to contribute nothing to the salinity value used to calculate

999   concentrations, but for constants, contributed 3, 2.5, 2, and 0.75 to the salinity for

1000 $NaHCO_3$, $NaHCO_3$/Na_2CO_3, Na_2CO_3, and Na_2CO_3 added during the period in which

1001   precipitation was occurring respectively. The use of 0.75 during precipitation reflects an

1002   assumption that for every unit of Na_2CO_3 added, a unit of $CaCO_3$ precipitates, thus

1003   reducing the overall change in salinity. Based on the measured final salinity, an

1004   evaporation rate was calculated to allow the expected salinity to match (within 0.1) the

1005   measured salinity. Using the salinity based evaporation rate the expected final mass was

1006   calculated, values were generally in good agreement with measured values (difference of

1007 1 ± 2 g (average $\pm$ standard deviation, excluding one suspect value)).

1008   To calculate carbonate chemistry and borate concentrations, a Matlab version of CO2sys

1009   (adapted from van Heuven et al., 2009, using constants from Mehrbach et al., 1973 as fit

1010   by Dickson and Millero 1987; Dickson 1990 for borate, and Dickson 1990 for sulfate)

1011   was used. In addition to the standard species considered, additional buffers were

1012   included (per alkalinity calculations, see above), and boron concentrations were

1013   calculated based on the boron:salinity relationship of Lee et al. (2010), plus any added

1014   boron when appropriate. Although nutrient chemistry was not measured in the seawater

1015   batches used in these experiments, previous studies have monitored nutrients in seawater

1016   from the same source (Holcomb et al., 2010; 2012), based on these data we assumed NH_3

1017 $= 0$, $H_2SiO_4 = 5$, and $PO_4 = 0.25$ μmol/kg sw at S=32 for all calculations. A wide range

1018   of species (SO_4^{2-}, F^-, etc.) are incorporated into aragonite and could influence the

1019   calculation of carbonate chemistry, however the likely effects were deemed insufficient

1020   to justify corrections in the calculation of carbonate chemistry (a typical S/Ca ratio

1021   measured in a synthetic precipitate was ~6 mmol/mol (unpublished data), which,

1022   assuming a concentration of 28 mmol SO_4^{2-}/kg sw represents less that 0.5% removed by

1023   the precipitate; for F, although a greater percentage of total F was removed (~5

1024   mmol/mol Tanaka et al., unpublished data), the low concentration present in seawater

1025   combined with the low pKa should result in little effect on alkalinity). Although the

1026   amount of boron removed by precipitation was trivial relative to measurement

1027   uncertainty, values were corrected by assuming the precipitate formed with a constant

1028   B/Ca ratio and the amount of precipitate formed corresponded to the difference between

1029   measured and expected (assuming no precipitation) alkalinity. Ca^{2+} values used to

1030   calculate saturation states were corrected for added calcium or calcium removed (based

1031   on the expected calcium concentration and the amount of calcium removed as estimated

1032   from alkalinity depletion). For a subset of experiments, solution $[Ca^{2+}]$ was measured

1033   (DeCarlo et al., 2015). Measured values showed similar patterns to calculated values,

1034   though measured values tended to be ~0.5 mmol/kg higher than expected.

1035

1036   *S3. ICPMS measurements*

1037   *S3.1. X-Series*

1038   Preparation of aragonite samples for measurement of B/Ca (and other element) ratios via

1039   Q-ICPMS (X-Series II, Thermo Fisher Scientific) followed standard protocols (Holcomb

1040   et al., 2015). Briefly powders were rinsed repeatedly with H_2O (18.2 MΩ, Millipore

1041   Integral 5), and most were cleaned with NaOCl. Cleaned powders were dried, weighed

1042   (~20 mg sub-sample), and dissolved in ~0.58 N HNO_3 (prepared from sub-boiling

1043 distilled (Savillex DST-1000) HNO_3), final acid concentration ~0.1 N. For X-Series

1044 measurements, samples were diluted in 2% HNO_3 containing various elemental spikes to

1045 a final concentration of ~100 ppm Ca or 10 ppm Ca, depending upon the elements to be

1046 measured (e.g. Zinke et al., 2014; Holcomb et al., 2015). The coral standard JCp-1 was

1047 used as the standard, with an accepted B/Ca ratio of 0.4596 mmol B/mol Ca (Hathorne et

1048 al., 2013).

1049 Ca measurements were also carried out on the X-Series using the same solutions used for

1050 measuring elemental ratios. Standards containing various concentrations of [Ca]

1051 (prepared from a 10000 ppm Ca standard (Fisher j/8240 lot 1147827)) were run to

1052 calibrate Ca count ratios relative to the Sc spike included in all solutions.

1053

1054 *S3.1.1. Sample purity*

1055 Aragonite is known to contain a wide range of cations and anions other than Ca^{2+} and

1056 CO_3^{2-}, with concentrations of each approaching 50 mmol/mol in aragonite formed in

1057 marine environments. Thus assuming just $CaCO_3$ is present may bias results. However,

1058 given our measurement reproducibility (~1.5%), fairly large changes in the composition

1059 of the sample would be needed before we would be able to identify a change in Ca. This

1060 is consistent with our measured calcium contents giving an average of 0.010 mol Ca/g

1061 sample, the value expected for pure $CaCO_3$. We thus considered the precipitates to be

1062 composed of pure $CaCO_3$ for calculations, though for illustration purposes we include

1063 one figure with B normalized to the measured Ca content in addition to mass based (Fig.

1064 S1).

1065

1066 *S3.2. MC-ICPMS*

1067 Boron in most samples was measured via MC-ICPMS (Neptune Plus, ThermoFisher

1068 Scientific or NU Plasma II, NU instruments). Cation and anion resin purification

1069 procedures were used for all aragonite samples (McCulloch et al., 2014), except the

1070 solutions were weighed to the nearest 0.00001 g to allow for more accurate calculation of

1071 B concentrations. A subset of samples was also prepared with the chemistry described in

1072 section S3.3. Boron concentrations were estimated based on the total B 10+11 intensity

1073 for the sample relative to bracketing standards of known [B]. B/Ca ratios in aragonite

1074 samples were calculated based on both the sample mass and the measured [Ca] (from X-

1075 Series measurements).

1076

1077 *S3.2.1. Agreement amongst B/Ca estimates*

1078 The validity of measurements of B/Ca ratios made using the X-Series could be

1079 compromised due to the use of the coral standard JCp-1 to calculate all ratios, despite

1080 some of the synthetic aragonites having B/Ca ratios substantially different from JCp-1

1081 (ranging from ~0.1 to 0.9 mmol/mol versus a value of 0.4596 mmol/mol for JCp-1).

1082 Although all measurements were made at similar Ca concentrations, B concentrations

1083 could deviate substantially from those of the standard, thus any non-linearity in the

1084 response could bias calculated ratios. To assess any potential bias in the X-Series

1085 measurements, B/Ca was also estimated from boron measurements made via MC-ICP-

1086 MS. Repeated measurements of B/Ca ratios made on different days via the X-Series

1087 gave a reproducibility (1 standard deviation) of 0.02 mmol B/mol Ca or better for any

1088 given sample, while MC-ICP-MS based measurements were reproducible to better than

1089   0.04 mmol B/mol Ca (1 standard deviation). In all cases the average standard deviation

1090   was less than 0.01 mmol/mol. Ratios determined with the X-Series differed from those

1091   determined via MC-ICP-MS. However, on average X-Series measurements were 0.016

1092   mmol/mol lower, which is within measurement error. The relationship between

1093   measurements made with the X-Series, and those made via MC-ICP-MS using different

1094   extraction and normalization approaches is shown in Fig. S1.

1095

1096   *S3.3. B purification chemistry using TRIS*

1097   Since seawater samples contain ions not efficiently removed by the cation/anion resins

1098   used for carbonate samples (Holcomb et al., 2014; McCulloch et al., 2014), the boron

1099   specific resin Amberlite IRA 743 was used to purify the B from solution. Although

1100   several protocols exist for purifying boron using this resin (e.g. Lecuyer et al., 2002;

1101   Lemarchand et al., 2002; Foster 2008; Trotter et al., 2011; Dissard et al., 2012), existing

1102   protocols require either careful control of pH during boron absorption to avoid the

1103   formation of precipitates, pre- or post-purification, or are conducted under low pH

1104   conditions at which the capacity of the resin to absorb boron is reduced. To avoid these

1105   problems, we used an organic buffer, TRIS (Tris(hydroxymethyl)aminomethane), to

1106   stabilize the pH during boron absorption at ~8, thus reducing problems with hydroxides

1107   precipitating yet allowing boron absorption to occur at relatively high pH, thus taking

1108   advantage of the absorption capacity of the resin. To a 5 ml polypropylene tube we

1109   added ~0.05 ml of pre-cleaned Amberlite resin (in 0.075 N HNO_3), 2.5 ml H_2O

1110   containing ~0.01 mg phenol red, varying amounts of sample (typically 0.1 ml, though for

1111   NaX solutions and other samples expected to have low [B] 0.4 ml were used), and TRIS

1112   buffer (0.5:1 to 2:1 ratio TRIS to sample volume, depending upon the nature of the

1113   sample). The TRIS buffer solution used was ~ 0.3 M TRIS (Acros 424571000 lot

1114   A0326538) prepared in ~ 0.07 N HNO_3 and stored in contact with Amberlite IRA 743

1115   resin. TRIS was prepared in dilute acid to limit the possibility of achieving too high a

1116   pH. Samples were incubated overnight on a shaker table, the supernatant discarded, resin

1117   rinsed 4x with H_2O, and then the boron eluted with 4 successive 0.6 ml volumes of 0.15

1118   N HNO_3 with at least 6 h incubation on the shaker table for each elution volume. In

1119   addition to solution samples, some precipitates and coral standards were also extracted

1120   following this protocol – precipitates were dissolved as described above prior to

1121   extraction. Nitric acid blanks were extracted as well to verify procedural blanks each

1122   time samples were extracted.

1123

1124   *S3.4. Validating TRIS extraction*

1125   To verify the veracity of the TRIS based extraction protocol, a number of samples were

1126   prepared using both the method described above as well as established techniques using

1127   either cation and anion column chemistry (McCulloch et al., 2014), or traditional

1128   amberlite based extraction techniques using NaOH to adjust the pH (e.g. Holcomb et al.,

1129   2014). Results show similar B/Ca ratios for aragonite samples prepared with the various

1130   methods (Fig. S1). Repeated measurements of seawater samples prepared with amberlite

1131   resin and TRIS gave a reproducibility of boron concentration estimates of better than 6%

1132   RSD, with an average reproducibility of 1.6% RSD. Measured seawater boron

1133   concentrations agreed with calculated concentrations with an average difference of

1134   <0.2%.

1135

1136   *S4. XRD and Raman*

1137   Verification of the mineral form present in all experiments run in 2013 was made via

1138   powder x-ray diffraction (XRD). Precipitates were loaded onto a Si holder on a rotating

1139   stage and diffraction patterns collected using a PANalytical Empyrean diffractometer (at

1140   the Centre for Microscopy, Characterisation & Analysis, UWA) using Ni filtered Cu Kα

1141   radiation (generator at 40 kV, current 40 mA). For reference purposes, a coral aragonite

1142   sample was run each day patterns were obtained for precipitates. A subset of

1143   experiments run in 2011 were characterized by XRD at WHOI by M. Sulanowska. A

1144   raman microscope was also used to determine the mineralogy of individual grains for

1145   many of the experiments per Holcomb et al. (2009) for experiments run in 2011; DeCarlo

1146   et al. (2015) for experiments run in 2013.

1147   In one experiment, in which precipitation was induced by adding a solution containing

1148   NaOH (experiment 11h) $Mg(OH)_2$ was likely formed, however no clear peaks associated

1149   with $Mg(OH)_2$ were detected with Raman nor XRD. Visual observation of the sample

1150   suggested aragonite was not the primary phase, and the elemental composition showed

1151   Mg/Ca ratios (~ 100x typical aragonite values) inconsistent with aragonite being the only

1152   phase present. Such observations point to a need for caution in relying on any single

1153   means of identifying the mineral phase formed in synthetic experiments – for instance,

1154   although XRD patterns for sample 11h were atypical (weak peak near $2\theta = 19^\circ$),

1155   aragonite peaks were clearly present (Fig. S2). Given the wide range of peak

1156   shapes/heights observed for different precipitates (likely reflecting variations in crystal

1157   sizes and orientations amongst experiments), the presence of a phase other than aragonite

1158   would not necessarily have been detected from an XRD pattern alone, particularly if a

1159   smaller range of scan angles targeting calcium carbonates were used.

1160

1161   *S5. Additional statistics*

1162   Since all temperature experiments represented pumping experiments without added B, K_D

1163   values from pumping experiments without added B conducted at ~25 ^{o}C were regressed

1164   against mean experimental saturation state and $[CO_3^{2-}]$ (variations in [B] were too small

1165   to justify inclusion). The regressions gave the following fits: K_D = -0.000865*Ω

1166   +0.0887, R^2 = 0.435 and K_D = 0.00000945*$[CO_3^{2-}]$ + 0.0856 R^2 = 0.343. Residuals (K_D

1167   – calculated K_D) were then calculated for all pumping experiments without added boron

1168   and plotted against temperature (Fig. S3). There was no trend in residuals with

1169   temperature regardless of the regression used, thus suggesting any effect of temperature

1170   on K_D is small relative to experimental variability. Equations 6 and 7 were also used for

1171   calculating the expected B/Ca ratio of each experiment, the difference between the

1172   measured and expected B/Ca ratio calculated, and again the values compared with

1173   temperature; no trend was detected. Tests for the effects of Tris, Hepes, and calcein were

1174   conducted in the same manner, regressions were calculated based on the full data-set

1175   (excluding experiments run in 2011, experiment 1c, and experiments containing Tris,

1176   Hepes, or calcein, (resulting equations: K_D = 0.0997 -0.0111*[B] -0.00111*Ω R^2=0.53,

1177   and K_D = 0.0945 -0.0124*[B] -0.0000116*$[CO_3^{2-}]$ R^2=0.55) residuals calculated and

1178   tested for significant (p<0.01) differences from 0 (t-test). In all cases, no significant

1179   differences were detected, though precipitates formed from solutions containing HEPES

1180   tended to have higher B/Ca than expected, while the opposite was observed for TRIS.

1181

1182   *S6. Effects of [Mg] and [Ca]*

1183   Since our experiments were conducted over a wide range of Ca and Mg concentrations,

1184   departing substantially from standard seawater conditions, there is the potential for the

1185   seawater based carbonate chemistry constants used in the main text to be inappropriate

1186   for our data. The inclusion of seawater carbonate chemistry constants in common

1187   programs used for calculating carbonate chemistry leads to their application in modeling

1188   biogenic calcification, and thus our choice to use them, however both Ca and Mg

1189   influence DIC and B speciation (Reardon 1976; Bassett 1980; Hain et al., 2015), thus

1190   taking such effects into account is essential for a robust treatment of our data. We

1191   modified CO2Sys to use the DIC (K_0, K_1, K_2), boric acid (K_B), water (K_W), hydrogen

1192   sulfate (K_{SO4}), and aragonite solubility constants of Hain et al. (2015). We further

1193   modified the MyAMI code of Hain et al. (2015) used to calculate these constants to

1194   include variable [H^+] (estimated from measured pH) and [$B(OH)_4^-$] (estimated with

1195   CO2Sys without corrections for Mg and Ca) for estimating Pitzer activity coefficients.

1196   To estimate what parameters are likely to be affected by [Mg] and [Ca], we calculated

1197   concentrations of different DIC species and borate using constants from Hain et al (2015)

1198   at both normal seawater [Mg] and [Ca] and ~2x elevated (Fig. S5). For B/DIC the

1199   change in constants had no effect, while for [$B(OH)_4^-$]/[CO_3^{2-}]$^{0.5}$ there was a slight

1200   influence. In contrast many of the individual DIC or B species show substantial effects

1201   (Fig. S5, S6), thus the relationship between B/Ca and individual chemical species is

1202   likely to change. Correlations between B/Ca and various solution chemistry parameters

1203   are presented in Table S3 and Figure S7 (a summary table with all solution chemistry

1204   parameters calculated using the adjusted constants is given in the supplemental data file).

1205   The use of different constants affected the correlations between B/Ca in the precipitate

1206   and some individual solution chemistry parameters (Table S3), however the strong

1207   correlations between B/Ca and mean $[B(OH)_4^-]/[CO_3^{2-}]^{0.5}$, [B]/[DIC] or $[B]/([CO_3^{2-}] +$

1208 $[HCO_3^-])$ and $[B(OH)_4^-]*[Ca^{2+}]$ remain consistent regardless of the constants used.

1209   Linear least squares regression (excluding experiment 1c for equations S1 and S2) using

1210   [Mg] and [Ca] corrected constants for solution chemistry calculations gave the following

1211   fits:

1212

1213   B/Ca (mmol/mol) = .0648 (±0.002) $[B(OH)_4^-]/[CO_3^{2-}]^{0.5}$ +.0359 (±0.013)   eq. S1

1214

1215   B/Ca (mmol/mol) = 2.795 (±0.133) [B]/[DIC] + 0.089 (±0.014)   eq. S2

1216

1217   B/Ca (mmol/mol) = 0.000148 (±0.000009) $[B(OH)_4^-]*[Ca^{2+}]$ + 0.0957 (±0.0178)   eq. S3

1218

1219   B/Ca (mmol/mol) = 0.001674 (±0.000144) $[B(OH)_4^-]$ + 0.0799 (±0.0253)   eq. S4

1220

1221   where $[B(OH)_4^-]$, $[CO_3^{2-}]$, [B], and [DIC] are in units of μmol kg sw^{-1}, $[Ca^{2+}]$ is in mmol

1222   kg sw^{-1} values in parentheses are 1 standard error, all parameter estimates were

1223   significant ($p \leq 0.001$, R^2=0.93 for eq. S1, R^2=0.89 for eq. S2, R^2=0.82 for eq. S3, and

1224 R^2=0.71 for eq. S4). Note that all coefficient estimates for eq. S1 and S2 are within one

1225   standard error of those in equations 4 and 5.

1226 Apparent partition coefficients (relationships based on [B]/[DIC], [B(OH)$_4^-$]*/[Ca^{2+}] and

1227 [B(OH)$_4^-$] are not for balanced reactions) of the form K = (B/Ca)/solution chemistry

1228 value were calculated for each experiment as described in the main text (Table S4). The

1229 K$_D$ values based on [B(OH)$_4^-$]/[CO$_3^{2-}$]$^{0.5}$ thus calculated tend to be slightly higher than

1230 those calculated without taking the effects of [Mg^{2+}] and [Ca^{2+}] into account, reflecting

1231 slightly lower [B(OH)$_4^-$]/[CO$_3^{2-}$]$^{0.5}$ ratios (Fig. S5)

1232

1233 Although we consider a K$_D$ expression based on [B(OH)$_4^-$]/[CO$_3^{2-}$]$^{0.5}$ to provide

1234 the best fit to our data, involve species likely incorporated into aragonite, as well as

1235 providing a charge balanced reaction, there are a number of apparent partitioning

1236 relationships which fit our data nearly as well, some of which have been suggested to be

1237 important by other authors, thus we present alternative fits for K$_D$ relationships. For the

1238 following fits all solution chemistry parameters were calculated using [Ca] and [Mg]

1239 corrected constants, experiment 1c was excluded for relationships based on [B(OH)$_4^-$

1240]/[CO$_3^{2-}$]$^{0.5}$ and [B]/DIC.

1241

1242 K = B/Ca/[B(OH)$_4^-$]/[CO$_3^{2-}$]$^{0.5}$ = -0.00008035 (0.0000158) [B(OH)$_4^-$] + 0.0878 (0.00278),

1243 R^2=0.32   eq. S5

1244

1245 K = B/Ca/[B(OH)$_4^-$]/[CO$_3^{2-}$]$^{0.5}$ = -0.00001634 (0.00000276) [CO$_3^{2-}$] -0.00001062

1246 (0.00000177) [B] +0.104 (0.004), R^2=0.49   eq. S6

1247

1248 $K = B/Ca/[B(OH)_4^-]/[CO_3^{2-}]^{0.5} = -0.001243\ (0.0002)\ \Omega\ -0.00001065\ (0.00000173)\ [B]\ +$

1249 $0.1072\ (0.00457)$, $R^2=0.51$ eq. S7

1250

1251 $K = B/Ca/[B]/DIC = -0.005306\ (0.001164)\ [B(OH)_4^-]-0.214\ (0.0275)\ [Ca^{2+}]+7.356$

1252 (0.385), $R^2=0.57$ eq. S8

1253

1254 $K = B/Ca/[B(OH)_4^-]*[Ca^{2+}] = -0.0000117\ (0.00000114)\ [Ca^{2+}] - 0.00000776$

1255 $(0.00000059)\ \Omega\ - 0.0000000462\ (0.00000000488)\ [B]\ +0.000535\ (0.0000197)$, $R^2 = 0.87$

1256 eq. S9

1257

1258 $K = B/Ca/[B(OH)_4^-] = -0.000001377\ (0.000000097)\ [CO_3^{2-}] - 0.0000003825$

1259 $(0.000000062)\ [B]+0.00433\ (0.00015)$, $R^2 = 0.79$ eq S10

1260 where $[B(OH)_4^-]$, $[CO_3^{2-}]$, $[B]$, and $[DIC]$ are in units of μmol kg sw^{-1}, $[Ca^{2+}]$ is in mmol

1261 kg sw^{-1} values in parentheses are 1 standard error, all parameter estimates were

1262 significant ($p \leq 0.001$). B/Ca ratios were calculated based on each of the above K_D

1263 expressions and compared to measured values (Table S5). Equations S6, S7, and S9

1264 provided the best fits. Residuals showed no significant effect of TRIS; for HEPES

1265 measured values were significantly ($p < 0.01$) higher than expected based on equation S9.

1266 Residuals from equation S8 were negatively correlated with temperature, whereas

1267 residuals from equations S3 and S4 were weakly positively correlated with temperature.

1268   Although in the full data set the correlation between B/Ca in the precipitate and

1269 $[B(OH)_4^-]*[Ca^{2+}]$ was nearly equivalent to correlations with $[B(OH)_4^-]/[CO_3^{2-}]^{0.5}$ and

1270   [B]/DIC, when data were separated by pumping vs degassing experiments, the use of

1271 $[B(OH)_4^-]*[Ca^{2+}]$ provided no improvement in the correlation relative to $[B(OH)_4^-]$ alone

1272   (e.g. Table 1). In contrast, $[B(OH)_4^-]/[CO_3^{2-}]^{0.5}$ was consistently more strongly

1273   correlated with B/Ca than $[B(OH)_4^-]$ alone. This suggests that rather than $[Ca^{2+}]$ being

1274   important in and of itself, it reflects a difference amongst degassing versus pumping

1275   experiments. Indeed $[Ca^{2+}]$ was generally higher in degassing experiments, while

1276   carbonate was generally lower (relative to pumping experiments) leading to a negative

1277   correlation between $[CO_3^{2-}]$ and $[Ca^{2+}]$ in both the overall data-set and certain subsets of

1278   the data. Thus we consider the strong correlation of B/Ca with $[B(OH)_4^-]*[Ca^{2+}]$ to

1279   reflect $[B(OH)_4^-]$ and a negative correlation between $[Ca^{2+}]$ and $[CO_3^{2-}]$ rather than an

1280   effect of $[Ca^{2+}]$.

1281

1282   **Supplemental References**

1283   **Bassett RL. 1980.** A critical evaluation of the thermodynamic data for boron ions, ion pairs,

1284   complexes, and polyanions in aqueous solution at 298.15 K and 1 bar. Geochimica et

1285   Cosmochimica Acta **44**:1151-1160 http://dx.doi.org/10.1016/0016-7037(80)90069-1.

1286   **Dickson AG. 1993.** pH buffers for sea water media based on the total hydrogen ion

1287   concentration scale. Deep-Sea Research **40**:107-118

1288   **Dickson AG, Millero FJ. 1987.** A comparison of the equilibrium constants for the dissociation of

1289   carbonic acid in seawater media. Deep-Sea Research **34**:1733-1743

1290   **Dickson AG, Wesolowski DJ, Palmer DA, Mesmer RE. 1990.** Dissociation constant of bisulfate

1291   ion in aqueous sodium chloride solutions to 250.degree.C. The Journal of Physical Chemistry

1292   **94**:7978-7985 10.1021/j100383a042.

1293   **Dissard D, Douville E, Reynaud S, Juillet-Leclerc A, Montagna P, Louvat P, McCulloch M.**

1294   **2012.** Light and temperature effect on d11B and B/Ca ratios of the zooxanthellate coral

1295   *Acropora sp.*: results from culturing experiments. Biogeosciences Discussions **9**:5969-6014

1296   10.5194/bgd-9-5969-2012.

1297   **Fofonoff N. 1985.** Physical Properties of Seawater A New Salinity Scale and Equation of State

1298   for Seawater. Journal of Geophysical Research **90**:3332-3342

1299   **Foster GL, Ni Y, Haley B, Elliott T. 2006.** Accurate and precise isotopic measurement of sub-

1300   nanogram sized samples of foraminiferal hosted boron by total evaporation NTIMS. Chemical

1301   Geology **230**:161-174 http://dx.doi.org/10.1016/j.chemgeo.2005.12.006.

1302   **Holcomb M, McCorkle DC, Cohen AL. 2010.** Long-term effects of nutrient and CO2 enrichment

1303   on the temperate coral Astrangia poculata (Ellis and Solander, 1786). J Exp Mar Biol Ecol

1304   **386**:27-33

1305   **Holcomb M, Cohen AL, McCorkle DC. 2012.** An investigation of the calcification response of

1306   the scleractinian coral *Astrangia poculata* to elevated pCO2 and the effects of nutrients,

1307   zooxanthellae and gender. Biogeosciences **9**:29-39 10.5194/bg-9-29-2012.

1308   **Holcomb M, Rankenburg K, McCulloch M. 2014.** High Precision MC-ICP-MS measurements of

1309   δ11B: matrix effects in direct injection and spray chamber sample introduction systems. . In:

1310   Grice, K (Ed), Principles and Practice of Analytical Techniques in Geosciences Royal Society of

1311   Chemistry, England, pp 251–270

1312   **Holcomb M, DeCarlo TM, Schoepf V, Dissard D, Tanaka K, McCulloch M. 2015.** Cleaning and

1313   pre-treatment procedures for biogenic and synthetic calcium carbonate powders for

1314   determination of elemental and boron isotopic compositions. Chemical Geology **398**:11-21

1315   http://dx.doi.org/10.1016/j.chemgeo.2015.01.019.

1316   **Lécuyer C, Grandjean P, Reynard B, Albarède F, Telouk P. 2002.** 11B/10B analysis of

1317   geological materials by ICP–MS Plasma 54: Application to the boron fractionation between

1318   brachiopod calcite and seawater. Chemical Geology **186**:45-55

1319   http://dx.doi.org/10.1016/S0009-2541(01)00425-9.

1320   **Lee K, Kim T-W, Byrne RH, Millero FJ, Feely RA, Liu Y-M. 2010.** The universal ratio of boron

1321   to chlorinity for the North Pacific and North Atlantic oceans. Geochimica et Cosmochimica Acta

1322   **74**:1801-1811 10.1016/j.gca.2009.12.027.

1323 **Lemarchand D, Gaillardet J, Göpel C, Manhès G. 2002.** An optimized procedure for boron

1324 separation and mass spectrometry analysis for river samples. Chemical Geology **182**:323-334

1325 http://dx.doi.org/10.1016/S0009-2541(01)00329-1.

1326 **McCulloch MT, Holcomb M, Rankenburg K, Trotter JA. 2014.** Rapid, high-precision

1327 measurements of boron isotopic compositions in marine carbonates. Rapid Communications in

1328 Mass Spectrometry **28**:2704-2712 10.1002/rcm.7065.

1329 **Mehrbach C, Culberson CH, Hawley JE, Pytkowicz RM. 1973.** Measurement of the apparent

1330 dissociation constants of carbonic acid in seawater at atmospheric pressure. Limnology and

1331 Oceanography **18**:897-907

1332 **Pawlowicz R. 2010.** A model for predicting changes in the electrical conductivity, practical

1333 salinity, and absolute salinity of seawater due to variations in relative chemical composition.

1334 Ocean Sci **6**:361-378 10.5194/os-6-361-2010.

1335 **Reardon EJ. 1976.** Dissociation constants for alkali earth and sodium borate ion pairs from 10 to

1336 50°C. Chemical Geology **18**:309-325 http://dx.doi.org/10.1016/0009-2541(76)90013-9.

1337 **Trotter J, Montagna P, McCulloch M, Silenzi S, Reynaud S, Mortimer G, Martin S, Ferrier-**

1338 **Pagès C, Gattuso J-P, Rodolfo-Metalpa R. 2011.** Quantifying the pH 'vital effect' in the

1339 temperate zooxanthellate coral *Cladocora caespitosa*: Validation of the boron seawater pH

1340 proxy. Earth and Planetary Science Letters **303**:163-173 10.1016/j.epsl.2011.01.030.

1341 **Zinke J, Rountrey A, Feng M, Xie SP, Dissard D, Rankenburg K, Lough JM, McCulloch MT.**

1342 **2014.** Corals record long-term Leeuwin current variability including Ningaloo Niño/Niña since

1343 1795. Nat Commun **5**10.1038/ncomms4607.

1344
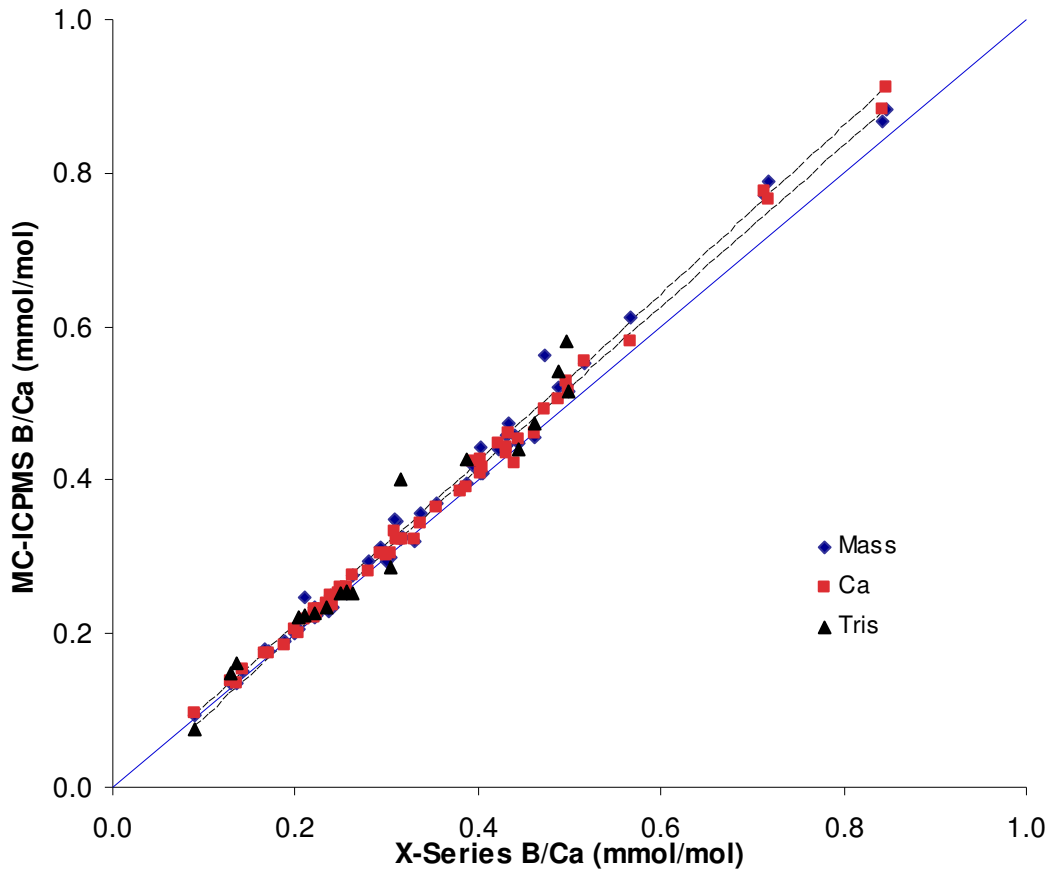
1345

1346   Figure S1. Relationship between different methods of determining B/Ca ratios. B/Ca

1347   ratios measured on the X-Series are plotted on the x-axis versus measurements made via

1348   MC-ICPMS (y-axis). Samples for which B (measured via MC-ICPMS) was extracted

1349   using column chemistry were normalized to Ca based on sample mass (blue diamonds),

1350   or measured Ca contents (red-orange squares). Samples for which B was extracted using

1351   Amberlite resin and TRIS buffer were normalized to Ca based on sample mass (black

1352   triangles). The 1:1 line is shown for reference (blue line). The relationship between the

1353   X-series measurements and MC-ICPMS measurements (normalized based on sample

1354   mass) was described by the following linear regression: B/Ca MC-ICPMS = B/Ca X-

1355   series *1.07 – 0.009 (R^2=0.99); the 95% confidence intervals for this regression are

1356   shown as dashed lines.

1357
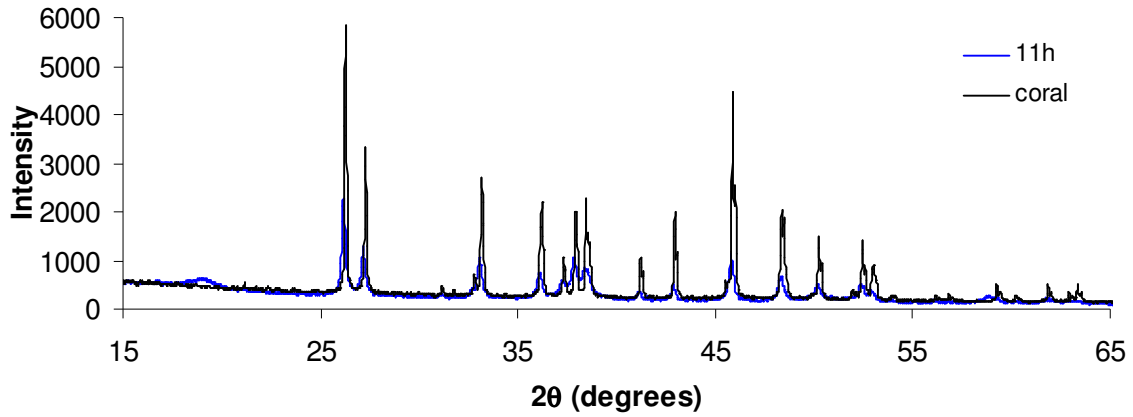
1358

1359   Fig S2. XRD patterns of a coral aragonite powder (black) and synthetic precipitate 11h

1360   (blue) containing a Mg rich phase in addition to aragonite.

1361
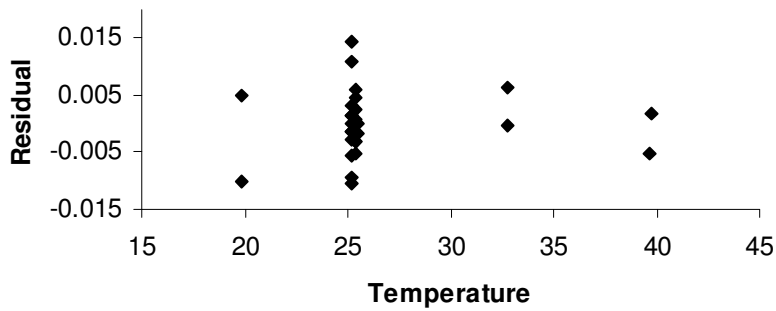
1362

1363   Figure S3. Residuals (experimental K_D – K_D calculated from $K_D = -0.000865*\Omega$

1364   +0.0887) plotted versus temperature for pumping experiments without added B.

1365
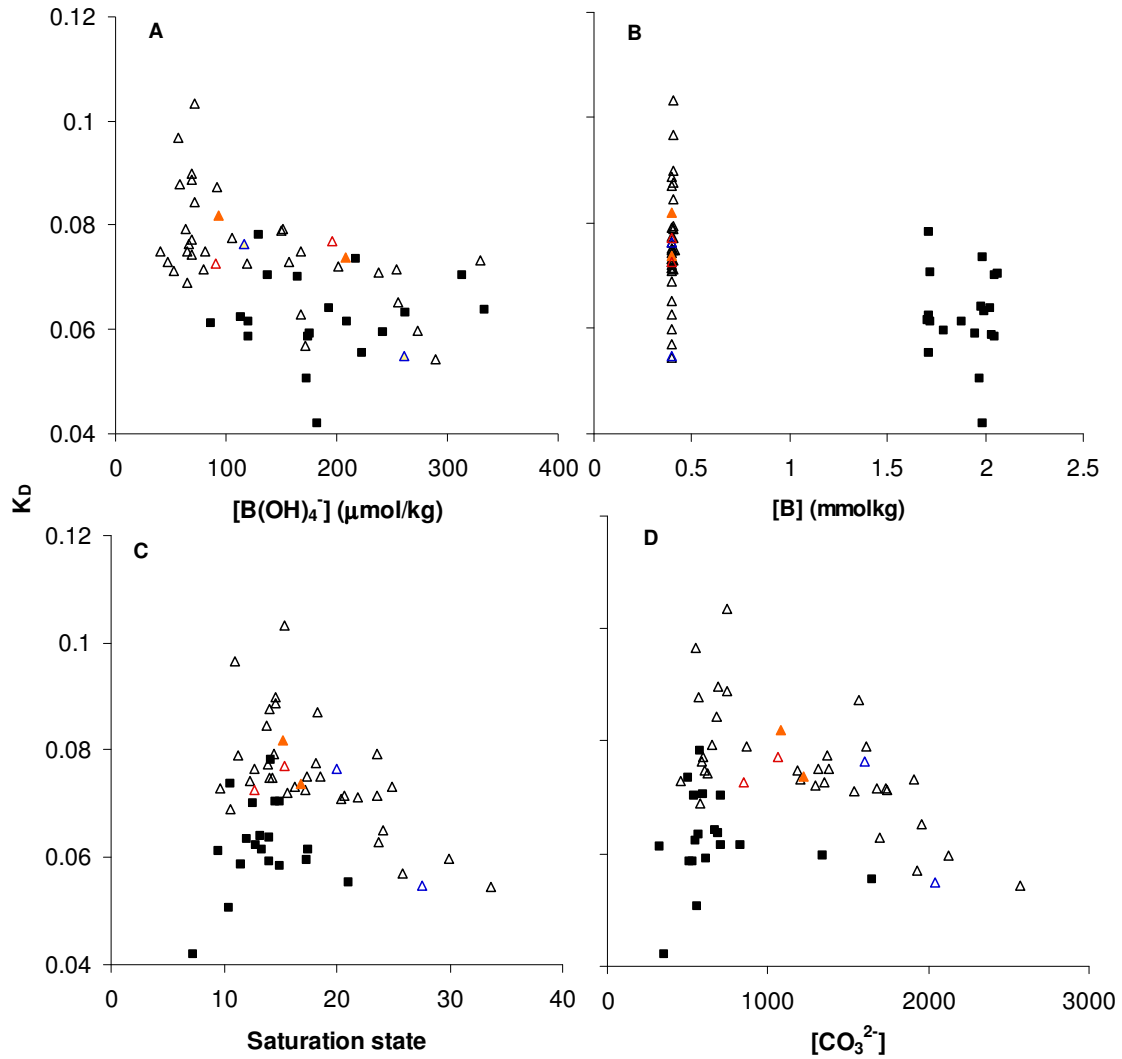
1366

Figure S4. Relationship between different solution chemistry parameters and K_D.

Symbols are means of individual experiments; experiments without added B are

represented by triangles, experiments with added B are represented by squares, error bars

are omitted for clarity. Experiments conducted at different temperatures are shown in

different colors: blue ~ 20, black ~ 25, orange ~ 33, and red ~ 40 ^{o}C. Most experiments

were conducted at ~ 25 ^{o}C, 2 experiments were run at each of the other temperatures.

1373

1374
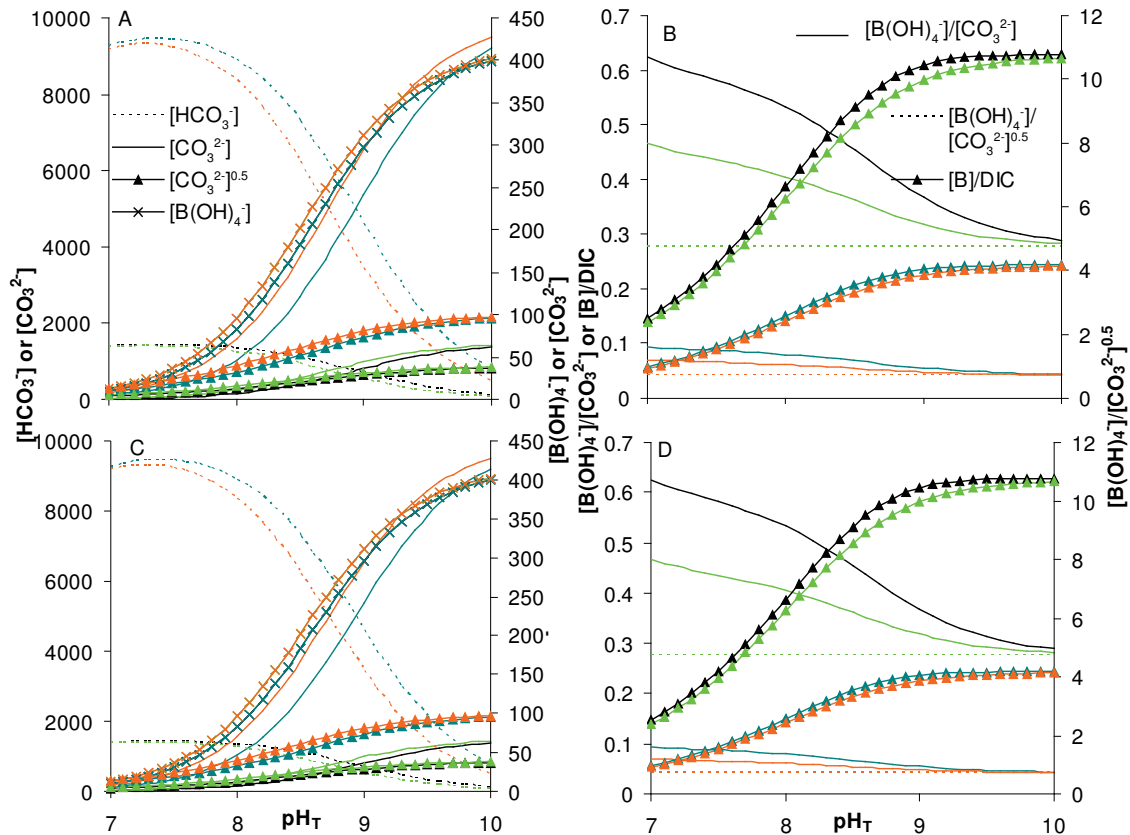
1375
1376 Figure S5. Relationships amongst DIC species as a function of pH calculated using

1377 constants from Hain et al. (2015). In A and B, two different DIC levels are used (1500 =

1378 black and green, 10000 = blue and orange); for each DIC, carbonate chemistry constants

1379 are calculated using the Pitzer model from the MyAMI code under standard seawater

1380 [Ca] and [Mg] (black and blue) or 2x [Ca] and [Mg] (green and orange). In C and D the

1381 same calculations are made but with additional corrections for the effects of pH

1382 variations on ion activity coefficients.

1383

1384

1385
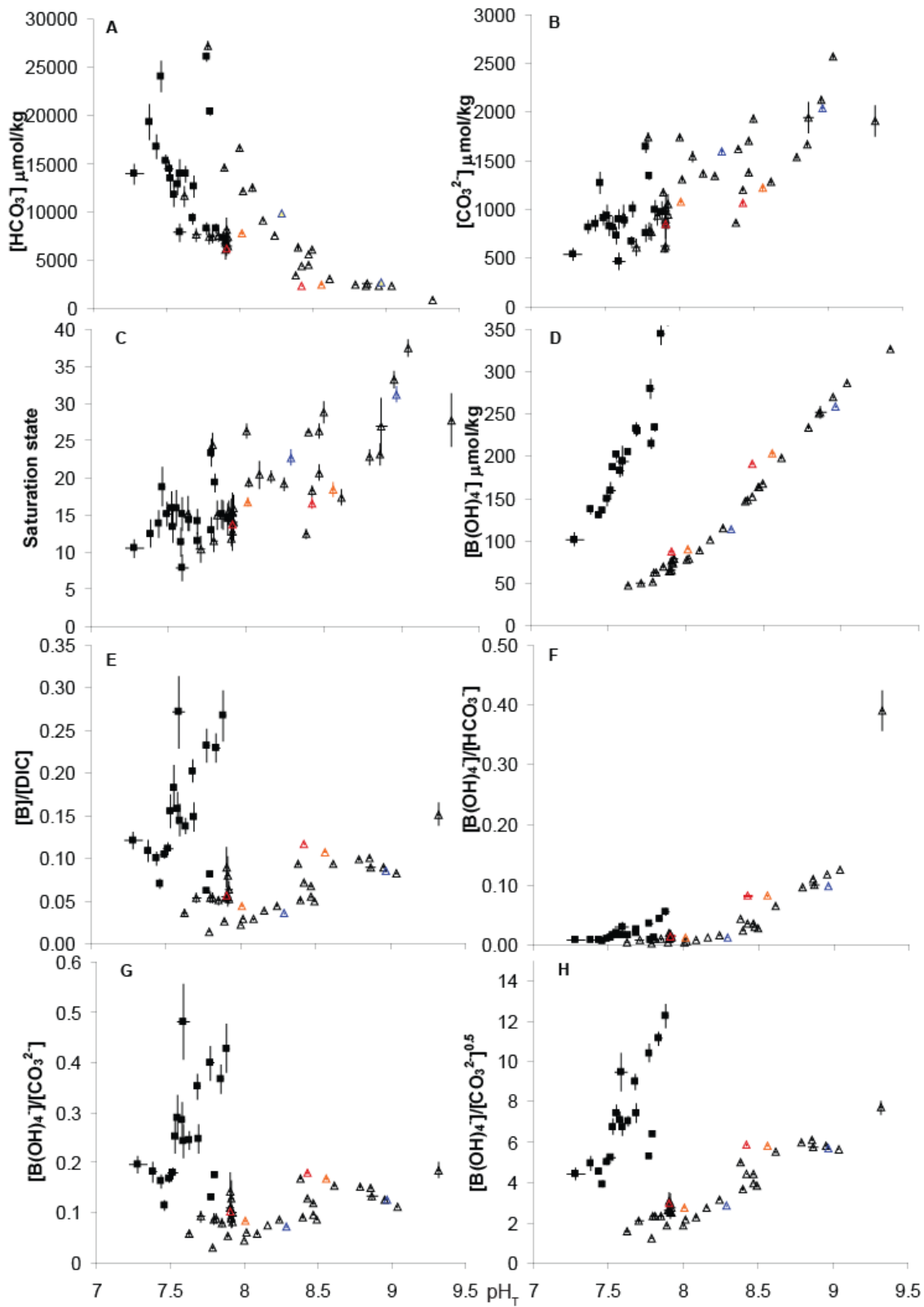
1386 Figure S6. Relationship between different solution chemistry parameters and pH_T as

1387 calculated using [Mg] and [Ca] corrected constants from Hain et al. (2015). Symbols are

1388 means of individual experiments; experiments without added B are represented by

1389 triangles, experiments with added B are represented by squares, lines show bi-direction

1390 error bars (1 sd). Experiments conducted at different temperatures are shown in different

1391 colors: blue ~ 20, black ~ 25, orange ~ 33, and red ~ 40 ^{o}C. Most experiments were

1392 conducted at ~ 25 ^{o}C, 2 experiments were run at each of the other temperatures.
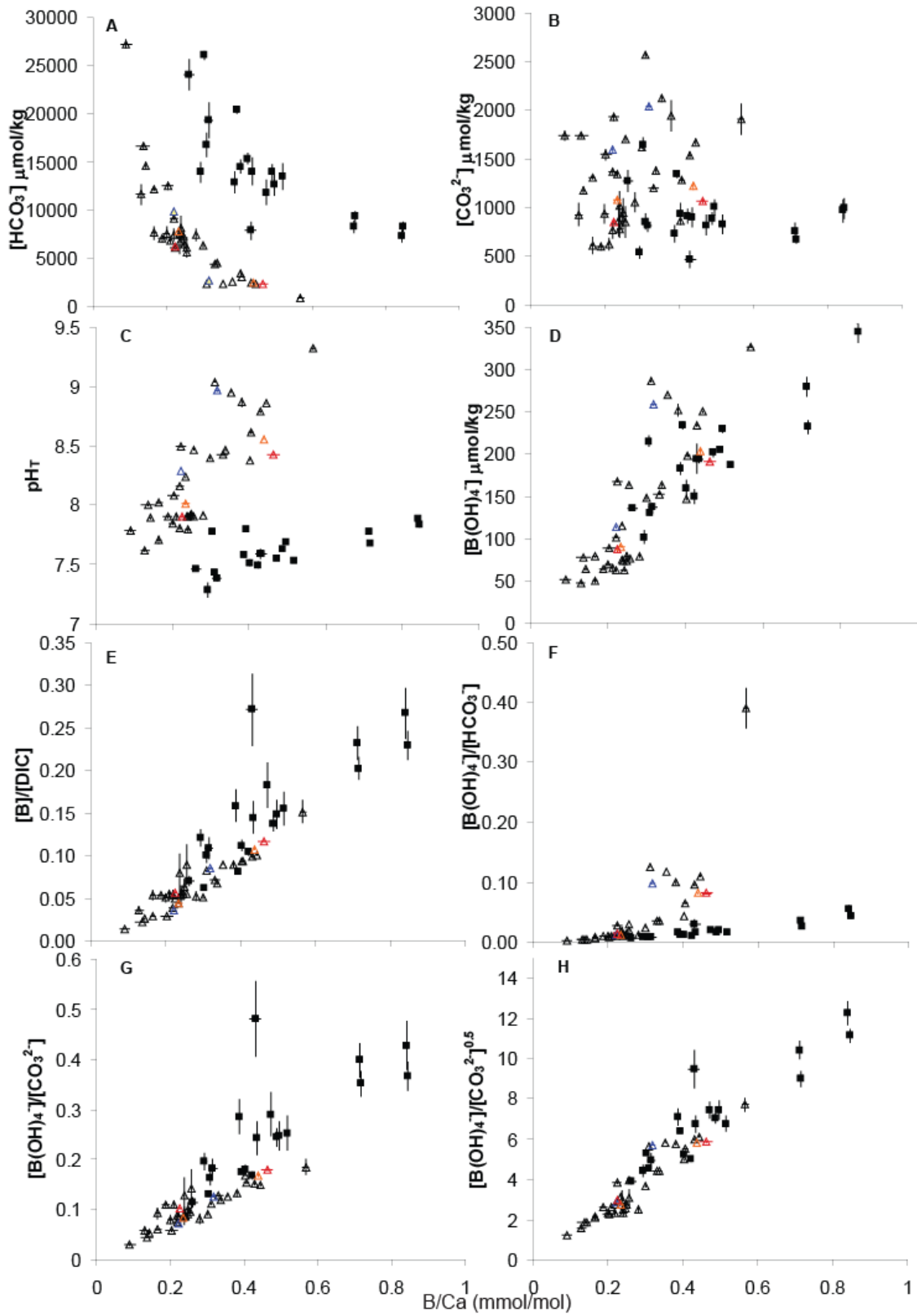
1393

1394   Figure S7. Relationship between B/Ca (mmol/mol) in aragonite and various solution

1395   chemistry parameters. Units for all species in solution are μmol/kg sw. Symbols are as

1396   described for Figure S6.

1397

1398

1399   Table S1. Experiment name, general description of precipitation approach used and any

1400   organic additives added. All experiments were carried out at 25 – 25.5 $^{\circ}$C unless

1401   specified otherwise. Those carried out at ~20 $^{\circ}$C are highlighted in blue, ~33 $^{\circ}$C in

1402   orange, ~40 $^{\circ}$C in red.

Experiment name/ precipitate	Description	Additives
1/19/11 a	Degassing, bubbled with air	calcein, OTC, alizarin
1/19/11 c	Degassing, bubbled with air	calcein
1/19/11 d	Degassing, bubbled with air	
1/19/11 f	Degassing, bubbled with air	
1/20/11 1	Pumping with Na_2CO_3	calcein, OTC
1/20/11 2	Pumping with Na_2CO_3	
1a	Degassing	
1c	Degassing with added B	
1e	Degassing with added B	TRIS
1f	Pumping with Na_2CO_3	
1g	Pumping with Na_2CO_3	
1h / ts20	Pumping with Na_2CO_3	
2a / ts9	Degassing, bubbled with air	
2b / ts8	Degassing, bubbled with air, added $CaCl_2$	
2c / ts6	Degassing, bubbled with air, added B	
2d / ts11	Degassing, bubbled with air, added B	HEPES
2e / ts5	Degassing, bubbled with air, added B	TRIS
2f / ts10	Pumping with Na_2CO_3/$NaHCO_3$, Na_2CO_3 during precipitation	
2g / ts1	Pumping with Na_2CO_3/$NaHCO_3$	
2h / ts2	Pumping with Na_2CO_3, 20 $^{\circ}$C	
3a / ts19	Degassing, bubbled with air	
3b / ts16	Degassing, bubbled with air	
3c / ts18	Degassing, bubbled with air, added B	
3d / ts17	Degassing, bubbled with air, added B	
3e / ts15	Degassing, bubbled with air, added B	TRIS
3f / ts12	Pumping with Na_2CO_3	
3g / ts3	Pumping with Na_2CO_3/$NaHCO_3$, Na_2CO_3 during precipitation	
3h	Pumping with Na_2CO_3, 33 $^{\circ}$C	
4a / ts26	Degassing, bubbled with air	
4b / ts33	Degassing, bubbled with air, added $CaCl_2$	
4c / ts28	Degassing, bubbled with air, added $CaCl_2$	
4d / ts29	Degassing, bubbled with air, added Na_2CO_3 and 2xsw	

4e / ts32	Degassing, bubbled with air, added Na_2CO_3	
4f / ts22	Pumping with $NaHCO_3$, Na_2CO_3 during precipitation	
4g / ts4	Pumping with $Na_2CO_3/NaHCO_3$, Na_2CO_3 during precipitation	
5a / ts41	Degassing, bubbled with ~5000 ppmv CO_2	
5b / ts39	Degassing, bubbled with ~5000 ppmv CO_2, added Na_2CO_3 and B	
5c / ts40	Degassing, bubbled with ~5000 ppmv CO_2, added $CaCl_2$ and B	
5d / ts42	Degassing, bubbled with ~5000 ppmv CO_2, added B	HEPES
5e / ts38	Degassing, bubbled with ~5000 ppmv CO_2, added B	TRIS
5f / ts24	Pumping with Na_2CO_3	
5g / ts14	Pumping with $NaHCO_3$, Na_2CO_3 during precipitation	
5h / ts7	Pumping with Na_2CO_3, 40 ^{o}C	
6a / ts54	Degassing, bubbled with ~15000 ppmv CO_2, added B	
6b / ts49	Degassing, bubbled with ~15000 ppmv CO_2, added $CaCl_2$ and B	
6c / ts52	Degassing, bubbled with ~15000 ppmv CO_2, added $NaHCO_3$ and B	
6d	Degassing, bubbled with ~15000 ppmv CO_2, added B	HEPES
6e / ts43	Degassing, bubbled with ~15000 ppmv CO_2, added B	TRIS
6f / ts50	Pumping with Na_2CO_3	
6g / ts23	Pumping with $NaHCO_3$, Na_2CO_3 during precipitation	
6h / ts13	Pumping with $NaHCO_3$, Na_2CO_3 during precipitation, 40 ^{o}C	
7g / ts25	Pumping with $NaHCO_3$, Na_2CO_3 during precipitation	
7h / ts21	Pumping with $NaHCO_3$, Na_2CO_3 during precipitation, 33 ^{o}C	
8f / ts44	Pumping with seawater containing $CaCO_3$ and $SrCO_3$ (dissolved with CO_2), bubbled with air	
8g / ts27	Pumping with $Na_2CO_3/NaHCO_3$, Na_2CO_3 during precipitation	
8h / ts31	Pumping with $NaHCO_3$, Na_2CO_3 during precipitation, 20 ^{o}C	

9g / ts30	Pumping with $NaHCO_3$, Na_2CO_3 during precipitation	
9h / ts37	Pumping with $NaHCO_3$, Na_2CO_3 during precipitation, bubbled with ~5000 ppmv CO_2	
10g / ts36	Pumping with $NaHCO_3$, Na_2CO_3 during precipitation, bubbled with ~2000 ppmv CO_2	
10h / ts45	Pumping with $NaHCO_3$, Na_2CO_3 during precipitation, added B	
11g / ts46	Pumping with $NaHCO_3$, Na_2CO_3 during precipitation, added B, bubbled with ~15 000 ppmv CO_2	
11h / ts48	Pumping with Na_2CO_3/NaOH	
12g / ts51	Pumping with Na_2CO_3	calcein
13g / ts53	Pumping with seawater containing $CaCO_3$ and $SrCO_3$ (dissolved with CO_2), bubbled with air	
13h / ts47	Pumping with Na_2CO_3/NaOH	

1403

Table S2. Summary of experimental chemistry during precipitation, B/Ca ratios in the precipitate, and K_D values. The standard deviation for solution chemistry values is given in the corresponding "sd" column. Experiments performed at different temperatures are in different colors: blue ~20 ^{o}C, black ~25 ^{o}C, orange ~33 ^{o}C, and red ~40 ^{o}C. TA, pH_T, and B/Ca (X-Series measurement) were measured, other values were calculated. For a subset of experiments B was also measured (see supplemental .xls file).

Exp.	pH_T	sd	TA (μmol/ kg)	sd	TC (μmol/ kg)	sd	HCO_3^- (μmol/ kg)	sd	CO_3^{2-} (μmol/ kg)	sd	Ω_{Arag}	sd	B (mmol/ kg)	sd	Borate (μmol/ kg)	sd	B/Ca (mmol/ mol)	Kd
1/19/11a	7.72	0.05	11575	1914	11103	1862	10376	1752	573	96	13.4	3.2	0.404	0.000	49	5	0.22	0.097
1/19/11c	7.61	0.05	11684	2057	11401	2038	10740	1933	450	74	10.5	2.5	0.405	0.000	39	5	0.16	0.080
1/19/11d	7.78	0.04	11358	1961	10794	1881	10033	1753	633	118	15.0	3.8	0.402	0.000	54	5	0.21	0.087
1/19/11f	7.64	0.05	11586	2066	11268	2054	10605	1953	468	64	10.8	2.2	0.405	0.000	42	5	0.18	0.085
1/20/11-1	8.33	0.04	4282	176	3486	86	2819	47	656	86	8.6	1.6	0.395	0.001	136	9	0.62	0.115
1/20/11-2	8.34	0.06	4015	129	3248	57	2614	76	624	80	8.4	1.4	0.395	0.000	138	12	0.58	0.105
1a	7.71	0.03	8890	808	8491	758	7924	696	458	64	9.6	1.6	0.403	0.000	47	3	0.17	0.073

1c	7.59	0.04	8992	1049	8609	1015	8105	950	351	64	7.3	1.7	1.988	0.001	183	16	0.43	0.042
1e	7.58	0.02	20294	1313	14021	1179	13222	1105	555	62	10.5	1.7	1.970	0.000	173	7	0.39	0.051
1f	8.61	0.01	5826	54	4313	36	3017	22	1291	19	15.6	0.9	0.400	0.000	202	1	0.41	0.072
1g	8.79	0.01	5813	65	3999	40	2454	20	1542	25	20.4	1.0	0.396	0.000	238	1	0.43	0.071
1h	8.86	0.01	5907	73	3932	44	2251	19	1679	28	20.7	1.3	0.397	0.000	254	1	0.44	0.072
2a	7.91	0.01	9152	852	8456	789	7703	714	687	71	14.5	1.9	0.404	0.000	69	1	0.25	0.090
2b	7.81	0.01	9019	784	8475	732	7826	669	565	59	14.0	1.8	0.404	0.000	57	1	0.22	0.088
2c	7.77	0.02	10045	754	9311	699	8639	638	570	62	12.1	1.7	1.994	0.000	263	11	0.71	0.063
2d	7.68	0.02	16782	778	10312	624	9663	588	508	33	10.6	1.0	1.990	0.000	217	7	0.72	0.074
2e	7.63	0.00	22300	915	15281	905	14377	852	668	39	13.2	1.2	1.977	0.000	194	2	0.49	0.064
2f	8.47	0.01	7492	100	5936	71	4544	48	1381	32	18.5	0.9	0.398	0.000	167	2	0.34	0.075
2g	8.40	0.01	9715	270	7956	253	6327	231	1611	23	23.6	0.2	0.399	0.000	152	2	0.30	0.079
2h	8.96	0.00	7034	62	4700	40	2656	19	2041	22	27.6	1.0	0.397	0.001	261	1	0.32	0.055
3a	7.92	0.01	9615	843	8855	784	8038	712	750	67	15.4	1.8	0.406	0.000	72	1	0.28	0.103
3b	7.79	0.02	9040	893	8521	852	7885	791	547	55	11.0	1.5	0.406	0.000	56	2	0.24	0.097
3c	7.88	0.02	9597	844	8637	763	7875	681	691	80	14.0	2.0	2.022	0.000	334	11	0.84	0.064
3d	7.84	0.02	10623	705	9689	632	8897	562	704	72	14.5	1.8	2.063	0.000	313	12	0.85	0.070
3e	7.69	0.01	21855	1166	14118	1241	13218	1170	709	51	13.3	1.5	1.877	0.000	209	4	0.50	0.061

3f	8.95	0.01	6876	67	4426	34	2299	3	2124	32	29.9	1.0	0.396	0.000	273	1	0.35	0.060
3g	8.43	0.00	6976	61	5614	46	4400	32	1201	17	16.3	0.6	0.397	0.000	157	1	0.33	0.073
3h	8.56	0.01	5174	63	3708	35	2484	11	1220	27	16.9	0.9	0.398	0.000	208	2	0.44	0.074
4a	7.92	0.02	8452	945	7750	851	7011	751	681	102	13.7	2.5	0.405	0.000	72	3	0.25	0.085
4b	7.90	0.00	7884	1337	7268	1243	6614	1130	597	104	13.9	2.7	0.405	0.000	69	0	0.26	0.077
4c	7.85	0.01	9536	819	8894	760	8161	690	654	67	14.4	1.9	0.406	0.000	63	2	0.20	0.079
4d	7.91	0.02	10246	1522	9502	1442	8677	1332	748	98	14.6	2.6	0.397	0.000	69	3	0.24	0.089
4e	7.91	0.02	8433	1503	7802	1412	7118	1294	620	106	12.4	2.5	0.400	0.000	69	2	0.24	0.074
4f	8.16	0.00	11956	136	10522	122	9111	107	1365	15	18.1	0.7	0.398	0.000	105	0	0.22	0.078
4g	8.47	0.00	9161	83	7294	64	5586	48	1695	21	23.6	0.9	0.398	0.000	167	1	0.26	0.063
5a	7.62	0.01	13509	1317	13058	1258	12258	1172	604	72	14.3	2.2	0.412	0.000	41	1	0.13	0.075
5b	7.59	0.01	16006	1586	15475	1555	14594	1468	617	61	14.1	2.0	1.949	0.000	175	3	0.43	0.059
5c	7.55	0.01	13669	1460	13217	1419	12466	1336	513	61	14.9	2.2	2.050	0.000	174	3	0.47	0.059
5d	7.53	0.01	19533	1550	14885	1476	14061	1393	537	57	12.5	1.9	2.046	0.000	164	2	0.52	0.070
5e	7.38	0.02	25217	1844	21058	1981	19938	1877	531	39	11.5	1.6	2.032	0.000	121	5	0.32	0.059
5f	9.04	0.00	7783	50	4855	25	2281	6	2573	24	33.7	1.1	0.397	0.000	290	1	0.31	0.054
5g	8.02	0.00	14910	180	13591	171	12194	160	1314	14	17.4	0.6	0.398	0.000	81	1	0.17	0.075
5h	8.43	0.01	4718	33	3406	20	2335	14	1066	14	15.3	0.7	0.399	0.000	196	1	0.46	0.077

6a	7.52	0.03	16546	884	16130	809	15220	747	593	68	14.9	2.1	1.724	0.000	138	9	0.40	0.071
6b	7.28	0.06	15110	1087	15331	1226	14368	1065	327	33	9.6	1.1	1.719	0.000	86	6	0.29	0.061
6c	7.44	0.01	18640	1395	18416	1372	17432	1296	546	50	12.8	1.7	1.715	0.000	114	2	0.31	0.062
6d	7.49	0.02	22684	1084	16951	639	16018	600	577	45	14.1	1.5	1.715	0.000	130	7	0.42	0.078
6e	7.46	0.01	31275	1792	26396	1744	24973	1648	829	64	17.5	2.4	1.703	0.000	120	2	0.26	0.062
6f	8.38	0.01	5348	42	4324	32	3446	27	868	13	11.2	0.6	0.402	0.000	150	2	0.40	0.079
6g	8.24	0.00	10397	146	8952	136	7573	125	1348	14	17.2	0.8	0.397	0.000	119	1	0.23	0.073
6h	7.91	0.01	7949	104	7033	92	6139	85	852	24	12.7	0.6	0.399	0.000	90	2	0.23	0.073
7g	8.00	0.00	20209	219	18509	211	16657	199	1733	18	23.6	0.9	0.399	0.000	79	1	0.14	0.072
7h	8.01	0.01	10056	110	8919	110	7793	108	1078	14	15.3	0.6	0.397	0.000	94	1	0.23	0.082
8f	7.90	0.03	8138	409	7545	363	6897	321	585	57	12.7	1.4	0.396	0.000	66	4	0.21	0.076
8g	8.49	0.01	10083	143	7974	114	6028	87	1932	34	25.8	1.3	0.397	0.000	172	1	0.22	0.057
8h	8.28	0.00	13102	185	11418	168	9777	149	1600	19	20.1	0.9	0.399	0.000	116	1	0.22	0.076
9g	7.79	0.01	30772	528	29287	503	27224	468	1746	42	21.9	1.4	0.402	0.000	53	1	0.09	0.071
9h	7.89	0.01	16954	402	15830	385	14510	360	1187	27	14.1	1.1	0.402	0.000	65	1	0.14	0.075
10g	8.09	0.01	15660	461	14071	428	12436	390	1562	41	18.3	1.6	0.398	0.000	92	1	0.20	0.087
10h	7.78	0.01	29597	532	28033	485	26074	441	1648	61	21.0	1.6	1.716	0.017	223	6	0.30	0.055
11g	7.80	0.01	23314	436	21955	419	20382	395	1343	26	17.3	1.1	1.790	0.028	242	4	0.39	0.060

12g	8.87	0.03	6744	306	4489	145	2530	10	1956	150	24.1	3.6	0.398	0.000	256	7	0.38	0.065
13g	7.90	0.01	8296	392	7711	363	7069	329	579	34	10.6	0.9	0.396	0.000	65	1	0.19	0.069
13h	9.32	0.01	5177	382	2809	227	895	72	1913	156	24.9	3.3	0.394	0.000	329	1	0.57	0.073

Table S3. Pearson correlation coefficients for mean solution chemistry parameters showing the most significant correlations with the B/Ca ratio of the precipitate, as well as various proposed ratios suggested to be linked to B/Ca regardless of significance. Correlation coefficients are given for the data set as a whole as calculated in the main text (Table 1), for calculations using the Pitzer model of Hain et al. (2015), and for calculations using the Pitzer model of Hain et al. (2015) taking into account the effects of [Mg] and [Ca].

Species in solution	Correlation with B/Ca (main text)	Correlation with B/Ca (Pitzer model)	Correlation with B/Ca (correcting for [Mg] and [Ca])
pH_T	0.03	0.03	0.03
$[HCO_3^-]$	-0.16	-0.16	-0.18
DIC	-0.18	-0.17	-0.18
$[B(OH)_4^-]^2/[CO_2][HCO_3^-]^2$	0.19	0.19	0.19
$[B(OH)_4^-]/[HCO_3^-]$	0.33	0.32	0.35
$[B(OH)_4^-]/([CO_3^{2-}] + [HCO_3^-])$	0.47	0.47	0.51
$[B(OH)_3]$	0.55	0.55	0.55
$[B(OH)_4^-]$	0.79	0.78	0.84

$[B]/[HCO_3^-]$	0.81	0.79	0.83
$[B(OH)_4^-]/[CO_3^{2-}]$	0.83	0.83	0.86
$[B]/([CO_3^{2-}] + [HCO_3^-])$	0.89	0.89	0.89
$[B]/[DIC]$	0.89	0.89	0.89
$[B(OH)_4^-]*[Ca^{2+}]$	0.92	0.92	0.91
$[B(OH)_4^-]/[CO_3^{2-}]^{0.5}$	0.95	0.95	0.95

Table S4. Apparent partition coefficients for potential relationships between B/Ca in the precipitate and solution chemistry parameters. Solution chemistry was calculated using constants from Hain et al. (2015) taking into account the effects of [Mg] and [Ca]. B/Ca is in mmol/mol, units are μmol/kg for all solution chemistry parameters except $[Ca^{2+}]$ which is in mmol/kg.

	$K = B/Ca/[B(OH)_4^-]/[CO_3^{2-}]^{0.5}$	$K = B/Ca/[B]/[DIC]$	$K = B/Ca/[B(OH)_4^-]*[Ca^{2+}]$	$K = B/Ca/[B(OH)_4^-]$
average K	0.0748	4.16	0.000227	0.00237
minimum K	0.0455	1.59	0.000123	0.00108
maximum K	0.111	7.12	0.000359	0.00388
standard deviation	0.0123	1.11	0.0000577	0.000645

Table S5. Mean absolute differences between measured and calculated B/Ca as calculated with equations S1-S10 relative to the measured value and standard deviation.

	S1	S2	S3	S4	S5	S6	S7	S8	S9	S10
mean	0.107	0.141	0.166	0.201	0.104	0.083	0.082	0.139	0.081	0.093
standard deviation	0.082	0.118	0.145	0.188	0.76	0.066	0.065	0.140	0.067	0.074

A supplemental .zip file is available which contains detailed data for each run, XRD patterns and/or Raman spectra for each precipitate, a full summary of precipitation chemistry and precipitate chemistry as determined with different measurement and extraction techniques.